Supplementary Material

Source-specific ecological and health risks of polycyclic aromatic hydrocarbons in the adjacent coastal area of the Yellow River Estuary, China

Authors: Zeyuan Li, Ruicheng Qi, Yufen Li, Jingjing Miao, Yaobing Li, Zhiheng He, Ning Zhang, Luqing Pan*

Address: The Key Laboratory of Mariculture, Ministry of Education, Ocean University of China, Qingdao 266003, PR China

***Corresponding author:**

Luqing Pan, Professor, Ph.D.

Tel.: +86 532 82032963;

Fax: +86 532 82032963;

E-mail address: panlq@ouc.edu.cn (L.Q. Pan)

Fisheries College, Ocean University of China,

Yushan Road 5, Qingdao 266003, China

Supplementary Methods

1. Determination of PAHs content in seawater, sediment, and clam soft tissue.

Chemicals, reagents, and solutions. The sixteen US-EPA priority PAH congeners (naphthalene (Nap), acenaphthylene (Acy), acenaphthene (Ace), fluorene (Flu), phenanthrene (Phe), anthracene (Ant), fluoranthene (Fla), pyrene (Pyr), benzo[a]anthracene (BaA), chrysene (Chr), benzo[b]fluoranthene (BbF), benzo[k]fluoranthene (BkF), benzo[a]pyrene (BaP), indeno[1,2,3-cd]pyrene (Ind), dibenzo[a,h]anthracene (DahA), and benzo[g,h,i]perylene (BghiP)) used for the determination of 16 PAHs in seawater, sediment and clam soft tissue, one internal standard 2,4,5,6-Tetrachloro-m-Xylene (TCMX) and five surrogates (i.e., Nap-d_8, Ace-d_{10}, Phe-d_{10}, perylene-d_{12}, and Chr-d_{12}) used for the determination of 16 PAHs in seawater, five internal standards (i.e., naphthalene-d8, phenanthrene-d10, acenaphthene-d10, perylene-d12, and chrysene-d12) and two surrogates (2-fluorobiphenyl and P-terphenyl-d14) used for the determination of 16 PAHs in sediment were obtained from J&K Scientific (Beijing, China). HPLC-grade n-hexane, dichloromethane and acetonitrile were obtained from Merck Inc. (Darmstadt, Germany), while methanol, acetone and copper powder were obtained Sinopharm Chemical Reagent (Shanghai, China). C18 (500 mg, 6 mL), Si (1 g, 6 mL), and Florisil (1 g, 6 mL) solid-phase extraction (SPE) cartridges were purchased from ANPEL Laboratory Technologies (Shanghai, China).

PAHs extraction and analysis. The pretreatment and quantification procedures of the sixteen US-EPA priority PAH congeners (naphthalene (Nap), acenaphthylene (Acy), acenaphthene (Ace), fluorene (Flu), phenanthrene (Phe), anthracene (Ant), fluoranthene (Fla), pyrene (Pyr), benzo[a]anthracene (BaA), chrysene (Chr), benzo[b]fluoranthene (BbF), benzo[k]fluoranthene (BkF), benzo[a]pyrene (BaP), indeno[1,2,3-cd]pyrene (Ind), dibenzo[a,h]anthracene (DahA), and benzo[g,h,i]perylene (BghiP)) were conducted as described in the Chinese National Standard Methods GB 26411-2010[1], HJ 805-2016[2], and GB 5009. 265-2016[3], respectively.

Seawater sample. The seawater samples were first filtered (0.45 μm), then, 500 mL seawater sample spiked with 20 ng d-IS were passed through a C18 cartridge (500 mg, 6 mL), which was preconditioned sequentially with dichloromethane, methanol, and ultrapure water (each with 10 mL). After sample loading, the cartridge was pumped under vacuum for 30 min to eliminate moisture, then it was eluted with dichloromethane (12 mL) and the elution rate was 1 drop/s. The elute was concentrated to near dryness and dissolved with 200 μL n-hexane prior to GC-MS/MS analysis. Quantification of the 16 priority PAHs in seawater samples was performed using a Shimadzu gas chromatography-mass spectrometry (GCMS-QP2020 NX, Shimadzu, Japan) equipped with a SH-Rxi-5Sil MS capillary column (30 m length × 0.25 mm i.d. × 0.25 μm film thickness). The initial oven temperature was set at 50℃ and was raised to 150℃ at a rate of 20℃/min (held for 2 min), and to 290℃ at a rate of 12℃/min (held for 7 min). The temperature of inlet, MS transfer line and ion source temperature were set at 250℃, 250℃ and 200℃, respectively. The injection volume was 1 μL in splitless mode. Helium gas was used as carrier gas with a constant flow of 1.5 mL/min. All targets were identified and quantified using selected reaction monitoring (SRM) mode with an electron ionization (EI) ion source. The analyte, retention time (min) and m/z for SIM were shown in the Table S15.

Sediment sample. The sediment samples were first pre-frozen at -20℃ for > 24 h, then were freeze-dried using a vacuum freeze drier (CoolSafe 55-4, SCANVAC, Denmark) at -48℃ and < 2.0 Pa (72

h) according to a recent study to quantify organic contaminants in ocean sediments[4], and then ground and sieved through a 100-mesh stainless-steel sieve. After that, 0.50 g copper powder was added to 2.00 g dry samples to eliminate sulfur, then the mixed samples spiked with 20 ng d-IS extracted with 15 mL acetone: n-hexane (1:1, v: v) by ultra-sonication, next, the mixture was centrifuged for 10 minutes at 4000 g. After extraction twice, the supernatant was concentrated, solvent exchanged (n-hexane/2 mL), and purified with Si SPE cartridge (1g, 6 mL), which was preconditioned with 5 mL dichloromethane and 10 mL n-hexane, then the 10 mL eluent (dichloromethane: n-hexane, 1: 9, v: v) was concentrated and finally redissolved with 200 μL n-hexane. Quantification of the 16 priority PAHs in sediment samples was performed using a Shimadzu gas chromatography-mass spectrometry (GCMS-QP2020 NX, Shimadzu, Japan) equipped with a SH-Rxi-5Sil MS capillary column (30 m length × 0.25 mm i.d. × 0.25 μm film thickness). The initial oven temperature was set at 80℃ for 2 min and was raised to 180℃ at a rate of 20℃/min (held for 5 min), and to 290℃ at a rate of 10℃/min (held for 5 min). The temperature of inlet, MS transfer line and ion source temperature were set at 280℃, 280℃ and 230℃, respectively. The injection volume was 1 μL in splitless mode. Helium gas was used as carrier gas with a constant flow of 1.0 mL/min. All targets were identified and quantified using selected reaction monitoring (SRM) mode with an electron ionization (EI) ion source. The analyte, retention time (min) and m/z for SIM were shown in the Table S16.

Clam sample. 1.00 g muscle tissue dry sample spiked with 20 ng d-IS were ultrasonically extracted twice with 20 mL acetonitrile and 10 mL n-hexane saturated acetonitrile, after centrifugation for 10 min at 6500 g, the fraction of acetonitrile was collected to concentrated by rotary evaporation and converted to 5 mL n-hexane, and purified in a Florisil SPE cartridge (1g, 6 mL), which was preconditioned with 5 mL dichloromethane and 10 mL n-hexane. Finally, the elution solution (dichloromethane:n-hexane, 1:1, 10 mL) was condensed and converted to n-hexane solution (200 μL) for GC-MS/MS analysis. Quantification of the 16 priority PAHs in clam samples was performed using a Shimadzu gas chromatography-mass spectrometry (GCMS-QP2020 NX, Shimadzu, Japan) equipped with a SH-Rxi-5Sil MS capillary column (30 m length × 0.25 mm i.d. × 0.25 μm film thickness). The initial oven temperature was set at 90℃ and was raised to 220℃ at a rate of 20℃/min, and to 320℃ at a rate of 5℃/min (held for 2 min). The temperature of inlet, MS transfer line and ion source temperature were set at 250℃, 280℃ and 230℃, respectively. The injection volume was 1 μL in splitless mode. Helium gas was used as carrier gas with a constant flow of 1.0 mL/min. All targets were identified and quantified using selected reaction monitoring (SRM) mode with an electron ionization (EI) ion source. The analyte, retention time (min) and m/z for SIM were shown in the Table S17.

Quality assurance and quality control. The determination of 16 PAHs in seawater, sediment and clam soft tissue were conducted under strict quality control and assurance procedures. Thus, solvent blanks, procedural blanks, spiked blanks, and triplicate samples were carried out for every batch of samples, and no target compounds were detected in the solvents or procedures (detailed results are shown in the Table S15-S17). Internal standard calibration was applied to quantify the PAH concentrations. The limits of detection (MDLs) of individual PAHs were calculated as being three times the signal versus noise value. The MDLs for seawater, sediment, and clam soft tissue samples were 0.020-0.196 ng/L, 0.018-0.176 and 0.029-1.186 ng/g, respectively (Table S15-S17). The spiked recoveries of 16 PAHs for seawater, sediment, and clam soft tissue samples ranged from 73±7% to 111±10%, 79±6% to 111±13% and 78±10% to 108±9%, respectively. Furthermore,

determined concentrations of Nap for all seawater and sediment samples and DahA, Ind for all seawater samples were below their MDLs, which were assigned as zero.

2. Biomarker analysis.

Biomarkers reflecting individual growth. Five conditions indices were measured to accurately determine the physiological condition of mussels (CI: condition index based on the wet weight, a.k.a., condition index; CIL: condition index based on the shell length; ST: shell thickness; GI: gonad index; HSI: hepato-somatic index). The CI was calculated using the ratio of the weight of soft tissue to the total weight (weight of soft tissue (g)/shell + soft tissues + pallet liquid (g)) of the mussel, multiplied by 100[5]. CIL is based on the shell length (weight of soft tissue (g)/the length of the shell[3] (mm) × 10^4 (g/mm)[6]. Shell thickness (ST) can be expressed as: (shell weight (g)/2)/(shell length (cm) × shell height (cm)), according to the relevant study[7]. Length was recorded as the distance from the umbo to the opposite shell margin and height was considered as the perpendicular to the length line. We also calculated two somatic body indices, according to the following equation: gonad index (GI) = weight of soft gonad (g)/shell + soft tissues + pallet liquid (g) × 100^8; hepato-somatic index (HSI) = weight of soft digestive gland (g)/shell + soft tissues + pallet liquid × 100 (g)[9].

Biomarkers in gills and digestive glands. After thawing, the digestive glands of the clams were homogenized in a phosphate buffer (0.125 M, pH 7.7, containing 0.05 M Na_2EDTA, 4°C) on ice for 3 min. The mixture was then centrifuged at 3000g for 25 min to remove the precipitate, followed by 12,000 g for 45 min at 4°C to separate the supernatants for the analysis of EROD, GST, T-AOC, SOD, CAT, GPx, GSH, LPO, DNA damage, PC content and AChE. EROD activity was measured using the modified method described previously[10], and the values were expressed as nmol/min/mg protein. The reaction mixture contained 10 mL 6 mM NADPH, 100 μL supernatant, 1.88 mL phosphate buffer and 10 μL 0.2 mM O7-ethylresorufin. After 10 min at 25°C, the reaction was terminated by adding 0.5 mL methanol. The O7-ethylresorufin fluorescence was measured at 560 nm/580 nm excitation/emission wavelengths using a spectrofluorometer (Molecular Spectroscopy LS 55, P.E., MA, USA).

GST activity was purified following a modification of the method described before[11]. The reaction mixture consisted of 200 μL 15 mM 1-chloro-2, 4-dinitrobenzene (CDNB), 200 μL 15 mM of reduced glutathione (GSH), 2 mL phosphate buffer, 200 μL supernatant and 400 μL H_2O. The reducing glutathione was incubated with CDNB at 25°C and the absorbance increase was measured at 340 nm (ε = 9.6/mM) using a spectrophotometer (Multiskan GO 1500, Thermofisher, USA) to determine the GST activity. The unit of GST activity was defined as nmol 2, 4-dinitrophenyl glutathione/mg protein/min.

The levels of T-AOC and reduced glutathione peroxidase (GSH) were detected using total antioxidant capacity assay kit (FRAP method, A015-3-1, Nanjing Jiancheng Bioengineering Institute, China) and reduced glutathione assay kit (A006-2-1, Nanjing Jiancheng Bioengineering Institute, China) according to the manufacturer's instructions, respectively. The spectrophotometer (Multiskan GO 1500, Thermofisher, USA) was used to measure the absorbance of samples and the contents of T-AOC capacity and reduced GSH were calculated by the respective standard curve.

SOD activity was detected using a modification of the method described in former research[12]. The reaction system contained 4.5 mL 50 mM Tris-HCl buffer (pH 8.3), 100 μL supernatant and 10 μL 50 mM pyrogallol. Oxidation of pyrogallol was determined by measuring the absorbance at 325 nm

with a spectrophotometer (Multiskan GO 1500, Thermofisher, USA). Based on the ability of SOD to inhibit the auto-oxidation of pyrogallol, the unit of SOD activity was defined as 50% inhibition of the oxidation process (U/mg protein).

CAT activity was measured according to the method described in relevant literature[13] and was based on the rate of decomposition of H_2O_2 by enzymes, monitoring the decrease in absorbance per minute at 240 nm with a UV spectrophotometer (Lambda 25, P.E., MA, USA). Briefly, the reaction system contained 2.9 mL 0.67 M 30% H_2O_2 and 100 μL sample. The concentration of H_2O_2 was determined at 25°C within 3 min. One unit of CAT activity was expressed as 50% H_2O_2 consumption per minute (U/mg protein/min).

The measurement of GPx activity was performed according to the method described in former work[14]. The reaction mixture consisted of 100 μL 1 mM glutathione (GSH), 0.2 mL 1.25 mM H_2O_2 and 400 μL supernatant. Each tube was maintained in a water bath at 37°C for 5 min, then 4 mL 50 g/L trichloroacetic acid was added to stop the reaction. After 10 min at 25°C, the solution was centrifuged at 3000 r/min for 10 min and then 2 mL of the supernatant was mixed with 2.5 mL 0.4 M Na_2HPO_4 (pH 10.0) and 0.5 mL 0.57 mM 5,5′-dithiobis-2-nitrobenzoic acid (DTNB) liquid, and the absorbance measured at 422 nm with a spectrophotometer (Multiskan GO 1500, Thermofisher, USA). The unit of GPx activity was expressed as consumption of 1 nmol GSH per minute at 37°C (nmol/mg protein /min).

Lipid peroxidation levels, expressed in terms of the MDA content, was measured using a practical approach[15]. The assay mixture consisted of 0.5 mL 0.67% thiobarbituric acid, 0.5 mL of tissue homogenate and 0.25 ml 20% TCA (including 1 mM $FeSO_4$). The mixtures were then incubated at 90°C for 10 min and centrifuged at 3000 r/min for 5 min. The absorbance at 412 nm was measured with a spectrophotometer (Multiskan GO 1500, Thermofisher, USA) and the results expressed as nmol MDA formed/min/mg proteins.

Protein carbonyl (PC) content was estimated by 2,4-dinitrophenylhydrazine (DNPH) assay[16] and expressed by the quantity of labeled protein hydrazones resulted from the reaction of DNPH and PC. The absorbance at 370 nm was measured with a spectrophotometer (Multiskan GO 1500, Thermofisher, USA) and the results were defined as nmol DNPH incorporated/mg protein based on the molar extinction coefficient of 22,000 M^{-1} cm^{-1}.

Acetylcholinesterase (AChE) activity was purified according to a widely applied method[17]. Tissues were homogenized in a phosphate buffer (0.1 M, pH 7.2) and then centrifuged at 10,000g for 20 min at 4°C. The reaction system contained 100 μL 10 mM 5,5′-dithiobis-2-nitrobenzoic acid (DTNB), 50 μL phosphate buffer, 50 μL sample and 20 μL 25 mM acetylthiocholine iodide. The absorbance at 412 nm was measured with a spectrophotometer (Multiskan GO 1500, Thermofisher, USA) and the AChE activity expressed in nmol thiocholine produced/min/mg protein using a molar extinction coefficient of 13.6 /(mM·cm).

The method to detect the DNA damage was according to relevant studies[18,19] with some modifications. In brief, DNA was extracted from the hemocytes before the assay of the DNA alkaline unwinding. Then the intact and highly polymerized DNA samples were divided into three equal parts to detect the fluorescence (excitation wavelength at 360 nm, emission wavelength at 450 nm) of double-stranded DNA (dsDNA), single-stranded DNA (ssDNA) and alkaline unwound DNA (auDNA) using a spectrofluorometer (Molecular Spectroscopy LS 55, P.E., MA, USA). The degree of DNA integrity was expressed by the F value: F value = (auDNA − ssDNA)/(dsDNA − ssDNA).

In accordance with the Bradford method[20], the total protein concentrations in gills, digestive glands

and hemocytes were determined by dye-binding and estimated by comparing the results with those for standard solutions of bovine serum albumin. The 50 μL supernatant was placed into each well and then 3.0 mL of Coomassie Brilliant Blue dye was added. The supernatant was gently but thoroughly mixed with the dye and allowed to stand for 10 min to enable it to react completely. The protein content was then calculated by measuring the absorbance at 595 nm with a spectrophotometer (Multiskan GO 1500, Thermofisher, USA).

Biomarkers in hemocytes. For the measurements of THC and cell viability, 100 μL hemocyte suspension was fixed with an equal volume of 10% formaldehyde (in order to observe better and prevent the rupture of hemocytes during the observation process) for 30 min at 4 °C, then added a drop of 3% Trypan blue[21]. A drop of the suspension was put in a hemacytometer, and THC was determined using an inverted phase contrast microscope (Olympus, Japan).

The phagocytic activity of hemocyte was measured using *Vibrio alginolyticus* according to the method described previously[22]. Hemocytes were isolated from 200 μL hemolymph and washed and resuspended with 1 mL saline solution by centrifugation at 700 g and 4°C, after which 100 μL hemocytes suspension and 100 μL bacterial suspension (1×10^7 cfu/mL) were loaded onto a plastic micro plate. The mixture was placed in the enzyme labelling instrument and incubated at 25°C for 30 min. A 50 μL mixed sample was then pipetted onto a glass slide and dried at 25 °C, stained with Giemsa stain for 15 min, decolorized in MilliQ water, and observed under an inverted phase contrast microscope (Olympus, Japan) (10 × ocular, 100 × oil immersion objective) after drying. Phagocytic activity was defined as: phagocytic rate (%) = (number of phagocytic hemocytes /200 hemocytes) × 100%.

The degree of lysosomal membrane stability was determined by the Neutral Red Retention (NRR) assay[23]. 200 μL hemocyte suspension was incubated with 20 μL neutral red solutions (0.33%) in dark at 10°C for 1 h. Following that, the mixture was centrifuged at 200 g for 10 min at 4°C. Sedimentation was washed twice with PBS after supernatant was removed. Aliquots (500 μL) of 1% acetic acid in 50% ethanol were added to the sedimentation at 20°C for 15 min. The absorbance at 550 nm was measured with a spectrophotometer (Multiskan GO 1500, Thermofisher, USA), and the results were expressed as the ratio between O.D. 550 nm and hemocyte protein.

Biomarkers in plasma. Antibacterial activity and bacteriolytic activity in plasma were measured using *Vibrio parahaemolyticus* and *Micrococus lysoleikticus*, respectively, modified from the method described in former study[24]. Briefly, 3 mL bacterial suspension (O.D. 570 nm = 0.3) prepared with sterile KH_2PO_4/K_2HPO_4 buffer (0.1 M, pH = 6.4) was added into a tube and placed in ice bath (0°C), then 100 μL plasma was added. The absorbance (A0) at 570 nm was measured immediately after vortex with a spectrophotometer (Multiskan GO 1500, Thermofisher, USA). Afterwards, the tube was incubated in water bath at 25°C for 30 min then returned to ice bath for 10 min to stop the reaction and the optical density at 570 nm (A) was measured again. The antibacterial activity and bacteriolytic activity, defined as U_a^2 and U_L, respectively, were calculated as follows:

$$U_a^2 = (A0-A)/A$$

$$U_L = (A0-A)/A$$

Gene expression analysis. Total RNA was isolated from gills using Trizol Reagent according to the manufacturer's instructions (Invitrogen, USA), and genomic DNA contamination was eliminated with RNase-free DNase (TaKaRa, Dalian, China). RNA samples were reverse-

transcribed using a Prime Script RT-PCR Kit (TaKaRa, China).

RT-PCR was used to detect the expression of 14 target genes (Table S18) and internal control gene (EF1A and RPS23). The primers were designed based on the GenBank sequence. The housekeeping gene EF1A and RPS23 were used as the control. Quantitative real-time PCR (qRT-PCR) was performed in a Thermo Scientific PikoReal 96-well Real-Time PCR System (Thermo Scientific., United States). The total amplification volume was 10 μL, including 5 μL of 2 × SYBR Green master Mix (TaKaRa, China), 1 μL of diluted cDNA, and 0.4 μL of each primer, and 3.2 μL of DEPC-treated water. The PCR program was as follows: denaturation program (95°C for 3min), amplification and quantification program repeated 40 times, melting curve program (60-95°C with a heating rate of 0.3°C per second), and finally cooled to 40°C. At the end of each PCR reaction, dissociation analysis of amplification products was performed to confirm that only one PCR product was amplified and detected. A control for deletion of the cDNA template was added to the qPCR analysis to determine the specificity of the target cDNA amplification.

After the PCR program, the data was analyzed using Thermo Scientific PikoReal software 2.1. The software automatically sets the baseline to maintain consistency. The comparative Ct method ($2^{-\Delta\Delta Ct}$ method)[25] was used to analyze the expression level of target genes.

3. Risk assessment

Risk quotient (RQ). The ecological risks of PAHs in seawater and sediment were assessed by the RQ method according to former studies[26,27]. The RQ of PAH congeners could be calculated by Eq. (1):

$$RQ = C_{PAHs}/C_{QV} \quad (1)$$

where, the C_{PAHs} was the concentration of certain PAHs in the medium and the C_{QV} was the corresponding quality values of certain PAHs in the medium. In this study, the negligible concentrations (NCs) and maximum permissible concentrations (MPCs) of PAHs in seawater and sediment were used as the quality values. Hence, the calculation formulas of RQ_{NCs} and RQ_{MPCs} were as Eqs. (2) and (3):

$$RQ_{NCs} = C_{PAHs}/C_{NCs} \quad (2)$$

$$RQ_{MPCs} = C_{PAHs}/C_{MPCs} \quad (3)$$

where, C_{NCs} was the quality values of the negligible concentrations of PAHs and C_{MPCs} is the quality values of the maximum permissible concentrations of PAHs in the medium. This method was improved by calculating the NCs/MPCs of six other PAH congeners based on the toxicity equivalent factor and proposed the equation to assess the ecological risks with PAH congeners fully considered[26]. The equations were as Eqs. (4)-(6):

$$RQ_{\sum PAHs} = \sum_{i=1}^{16} RQ_i \ (RQ_i \geq 1) \quad (4)$$

$$RQ_{\sum PAHs(NCs)} = \sum_{i=1}^{16} RQ_{i(NCs)} \ (RQ_{i(NCs)} \geq 1) \quad (5)$$

$$RQ_{\sum PAHs(MPCs)} = \sum_{i=1}^{16} RQ_{i(MPCs)} \ (RQ_{i(MPCs)} \geq 1) \quad (6)$$

where, $RQ_{(NCs)}$ and $RQ_{(MPCs)}$ of PAH congeners, which were not less than 1, were summated to calculate the $RQ_{\sum PAHs(NCs)}$ and $RQ_{\sum PAHs(MPCs)}$ of ∑PAHs[27]. Based on the values of $RQ_{(NCs)}$ and $RQ_{(MPCs)}$ for PAH congeners and values of $RQ_{\Sigma PAHs(NCs)}$ and $RQ_{\Sigma PAHs(MPCs)}$ for ΣPAHs, each site was categorized to various degrees of ecological risks, that ranged from risk-free to high risk (Table S10).

Incremental lifetime cancer risk (ILCR). The ILCR approach was applied to evaluate the carcinogenic effects related to dietary intake of PAHs in seafood. The cancer risks were assessed using the following equation[28]:

$$ILCR = TEQ \times CR \times EF \times ED \times SF \times CF/(BW \times AT) \quad (7)$$

In Eq. (7), the total toxic equivalency (TEQ) of 16 PAHs detected in clams were calculated using Eq. (8).

$$TEQ = \sum_{i=1}^{n} C_i \times TEF_i \quad (8)$$

In Eq. (8), TEF_i is the toxic equivalent factor of each individual PAH congener i relative to that of Benzo[a]pyrene (BaP) and C_i is the concentration of this compound in the clams. The calculated TEF values were listed in Table S14 according to former research[29].

In Eq. (7), where ILCR is the incremental lifetime cancer risk, CR is the ingestion rate of seafood (g/day), which is taken to be 13.7 and 6.3 g/day for urban and rural residents in Shandong based on Shandong Statistical Yearbook 2022[30]; EF is the exposure frequency (365 day/year); ED is the exposure duration (70 years for adults' average life expectancy); SF is the oral cancer slope factor for BaP of 7.3 $(mg/kg/day)^{-1}$; CF is the conversion factor (1.0×10^{-6} mg/ng); AT is the average lifespan for carcinogens (25, 550 days) and BW is body weight (kg), which was set at 70 kg for the average adult body weight[31]. According to the guidelines recommended by the US-EPA, ILCR below 10^{-6} is considered to be a negligible risk; if the ILCR reaches 10^{-6} and below 10^{-4}, it is assumed to pose a low risk in food that is acceptable; if the ILCR is up to or greater than 10^{-4}, this indicates that the PAH residue in food is of unacceptable and high risk that requires urge attention[32].

Integrated biomarker response (IBR). In this study, we employed integrated biomarker response (IBR) to assess the responses of multiple biomarkers (ST, EROD, GST, SOD, CAT, GPx, LPO, AChE, HSP22-2) in clams *R. philippinarum* and *M. veneriformis*. The method established by Beliaeff and Burgeot[33] was used, and the detailed calculation process was as follows: (1) Calculation of the mean (x_i) and standard deviation (s) of each site for each biomarker, as well as the mean (x) of all sites. (2) Standardization of data for each site: $y_i = (x_i\text{-}x)/s$, where y is the standardized value of the biomarker. (3) Calculation of z for each biomarker: $z = y_i + |\min y_i|$ if the biomarker is activated by contaminants, or $z = -y_i + |\min y_i|$ if the biomarker is inhibited by contaminants, where $\min y_i$ is the minimum value for all sites for each biomarker. (4) The radius coordinate in the star plots represents the z value for each biomarker in a certain site. $A_i = 1/2 \cdot \sin(2\pi/n) \cdot y_i \cdot y_{i+1}$, $IBR = \Sigma A_i$, where y_i and y_{i+1} represent the scores of a certain biomarker and its successive star plot radius coordinates, and n represents the number of biomarkers used in this study. Since the IBR value is

directly dependent on the number of biomarkers in the dataset, the obtained IBR value was divided by the number of biomarkers used to calculate IBR/n[34].

Multi-biomarker pollution index (MPI). The MPI approach was calculated according to the original research[35]. The measured values of each biomarker at each station were processed and the following values were calculated. The value of MPI of each site is calculated as follows:

$$MPI = \sum_{j=1}^{n} BPI_j \quad (9)$$

In Eq. (9), where j is the value of each biomarker and BPI represents the biomarker pollution index (Table S19), which is related to the discriminatory factor (DF):

$$DF = (X_{max}\text{-}X_{min}+CI)/CI \quad (10)$$

In Eq. (10), where X_{max} and X_{min} mean the maximum and minimum value, respectively. CI is the average confidence interval at the significance level of 0.05. Based on the value of MPI, the pollution status can be divided into five levels: red (> 50, highly polluted), orange (40-50, moderately polluted), yellow (30-40, lightly polluted), green (20-30, generally favorable) and blue (<20, clean).

4. Positive matrix factorization (PMF) model

In this study, the PMF model was used to quantify the sources apportionment of PAHs, and the basic formula is Eq. (11):

$$x_{ij} = e_{ij} + \sum_{j=1}^{P} g_{ik} f_{kj} \quad (11)$$

Where the x_{ij} is a matrix of i by j denoting the j-th species concentrations of sample i. The e_{ij}, g_{ik} and f_{kj} represent the residue error matrix, the factor contribution matrix and factor profile matrix. The k marks the decomposed source factor. The p means the different sources of PAHs, and all sample data were analyzed by the software EPA PMF 5.0[36]. The minimizing objective function Q summed all sample residuals and their uncertainties to optimize the PMF model, as Eq. (12):

$$Q = \sum_{i=1}^{n}\sum_{j=1}^{m}\left(\frac{e_{ij}}{u_{ij}}\right)^2 \quad (12)$$

Where n and m are the numbers of sample and the species of PAH in this study, respectively. The u_{ij} marks the uncertainty in the x_{ij}. According to the relevant study[37], the calculated equations are Eq. (13) and Eq. (14):

$$u_{ij} = \frac{5}{6} \times MDL_{ij}, \ x_{ij} < MDL_{ij} \quad (13)$$

$$u_{ij} = \sqrt{\left(EF_{ij} \cdot x_{ij}\right)^2 + \left(0.5 \times MDL_{ij}\right)^2}, \ x_{ij} \geq MDL_{ij} \quad (14)$$

Where the MDL stands for the method detection limit of PAHs, and the EF is the error fraction. In this study, the EF is regarded as a constant of 10%[38].

Supplementary Tables

Table S1 The contribution rate (RQ_i) of the RQ of i-th PAH for the sum of RQ in each site.

PAHs	RQ_i of PAHs in seawater				RQ_i of PAHs in sediment			
□	S1	S2	S3	S4	S1	S2	S3	S4
Acy	0.029	0.041	0.033	0.020	0.148	0.208	0.147	0.129
Ace	0.013	0.015	0.012	0.007	0.060	0.041	0.061	0.019
Flu	0.025	0.040	0.026	0.018	0.009	0.008	0.006	0.005
Phe	0.025	0.030	0.018	0.018	0.150	0.137	0.107	0.073
Ant	0.011	0.012	0.008	0.006	0.064	0.042	0.054	0.028
Fla	0.024	0.009	0.008	0.006	0.010	0.011	0.011	0.017
Pyr	0.109	0.077	0.088	0.042	0.417	0.360	0.385	0.375
BaA	0.344	0.191	0.109	0.078	0.038	0.036	0.047	0.107
Chr	0.016	0.014	0.007	0.004	0.003	0.003	0.004	0.004
BbF	0.297	0.435	0.574	0.668	0.083	0.135	0.163	0.214
BkF	0.009	0.014	0.019	0.030	0.001	0.004	0.003	0.003
BaP	0.070	0.099	0.089	0.094	0.013	0.012	0.011	0.022
DahA	-	-	-	-	0.001	0.002	0.002	0.002
Ind	-	-	-	-	0.001	0.001	0.001	0.001
BghiP	0.028	0.023	0.010	0.008	0.001	0.000	0.001	0.001

Table S2 The contribution rate (SF_{ij}) of the i-th PAH for the j-th factor (correspond to the j-th source) of PMF, in this study, which was derived from the PMF model. The "F" represented the factor derived from PMF model.

PAHs	SF_{ij} of PAHs in seawater				SF_{ij} of PAHs in sediment			
□	F1	F2	F3	F4	F1	F2	F3	F4
Acy	0.021	0.026	0.012	0.018	0.011	0.020	0.023	0.023
Ace	0.010	0.029	0.031	0.006	0.008	0.032	0.010	0.027
Flu	0.015	0.016	0.038	0.008	0.005	0.036	0.008	0.028
Phe	0.007	0.006	0.045	0.019	0.021	0.049	0.002	0.005
Ant	0.008	0.005	0.037	0.027	0.050	0.008	0.008	0.011
Fla	0.004	0.014	0.020	0.039	0.041	0.009	0.010	0.017
Pyr	0.012	0.009	0.023	0.033	0.031	0.017	0.015	0.014
BaA	0.007	0.016	0.022	0.033	0.037	0.014	0.008	0.017
Chr	0.034	0.008	0.004	0.030	0.037	0.008	0.020	0.012
BbF	0.039	0.013	0.007	0.018	0.013	0.013	0.035	0.015
BkF	0.040	0.019	0.010	0.007	0.015	0.015	0.033	0.014
BaP	0.042	0.015	0.003	0.017	0.008	0.008	0.053	0.009
DahA	-	-	-	-	0.013	0.010	0.034	0.019
Ind	-	-	-	-	0.009	0.015	0.036	0.018
BghiP	0.045	0.022	0.008	0.002	0.019	0.015	0.032	0.010
Total	0.284	0.198	0.258	0.259	0.318	0.269	0.328	0.239

Table S3 RQ_{PMF}^{i} was the calculated value of ecological risk of PAH individuals to contribution of the j-th source in seawater. The total RQ_{PMF}^{j} ($T^{RQ_{PMF}^{j}}$) was sum of the RQ_{PMF}^{i} for 16 PAHs, which was the contribution rate of j-th source to the ecological risk. The "F" represented the pollution source.

PAHs in seawater	RQ_{PMF}^{i} of S1				RQ_{PMF}^{i} of S2				RQ_{PMF}^{i} of S3				RQ_{PMF}^{i} of S4			
	F1	F2	F3	F4	F1	F2	F3	F4	F1	F2	F3	F4	F1	F2	F3	F4
Acy	0.008	0.010	0.005	0.007	0.011	0.014	0.006	0.010	0.009	0.011	0.005	0.008	0.005	0.007	0.003	0.005
Ace	0.002	0.005	0.005	0.001	0.002	0.006	0.006	0.001	0.002	0.004	0.005	0.001	0.001	0.003	0.003	0.001
Flu	0.005	0.005	0.012	0.003	0.008	0.008	0.019	0.004	0.005	0.005	0.013	0.003	0.004	0.004	0.009	0.002
Phe	0.002	0.002	0.015	0.006	0.003	0.003	0.018	0.008	0.002	0.002	0.011	0.005	0.002	0.001	0.010	0.004
Ant	0.001	0.001	0.005	0.004	0.001	0.001	0.006	0.004	0.001	0.001	0.004	0.003	0.001	0.000	0.003	0.002
Fla	0.001	0.004	0.006	0.012	0.000	0.002	0.002	0.005	0.000	0.001	0.002	0.004	0.000	0.001	0.002	0.003
Pyr	0.018	0.013	0.032	0.047	0.012	0.009	0.023	0.033	0.014	0.010	0.026	0.038	0.007	0.005	0.012	0.018
BaA	0.030	0.070	0.098	0.147	0.017	0.039	0.054	0.082	0.010	0.022	0.031	0.046	0.007	0.016	0.022	0.033
Chr	0.007	0.002	0.001	0.006	0.006	0.002	0.001	0.005	0.003	0.001	0.000	0.003	0.002	0.000	0.000	0.002
BbF	0.152	0.049	0.026	0.070	0.223	0.072	0.038	0.102	0.294	0.095	0.050	0.135	0.342	0.111	0.058	0.157
BkF	0.005	0.002	0.001	0.001	0.007	0.004	0.002	0.001	0.010	0.005	0.002	0.002	0.016	0.008	0.004	0.003
BaP	0.038	0.014	0.003	0.016	0.054	0.019	0.004	0.022	0.048	0.017	0.003	0.020	0.051	0.018	0.003	0.021
BghiP	0.016	0.008	0.003	0.001	0.013	0.006	0.002	0.001	0.006	0.003	0.001	0.000	0.005	0.002	0.001	0.000
$T^{RQ_{PMF}^{j}}$	0.285	0.184	0.211	0.320	0.357	0.183	0.181	0.278	0.403	0.177	0.153	0.267	0.441	0.177	0.131	0.251

Table S4 RQ_{PMF}^{i} was the calculated value of ecological risk of PAH individuals to contribution of the j-th source in sediment. The total RQ_{PMF}^{j} ($T^{RQ_{PMF}^{j}}$) was sum of

the RQ_{PMF}^{i} for 16 PAHs, which was the contribution rate of j-th source to the ecological risk. The "F" represented the pollution source.

PAHs in seawater	RQ_{PMF}^{i} of S1				RQ_{PMF}^{i} of S2				RQ_{PMF}^{i} of S3				RQ_{PMF}^{i} of S4			
	F1	F2	F3	F4	F1	F2	F3	F4	F1	F2	F3	F4	F1	F2	F3	F4
Acy	0.021	0.038	0.044	0.045	0.029	0.054	0.061	0.063	0.021	0.038	0.043	0.045	0.018	0.034	0.038	0.039
Ace	0.006	0.025	0.008	0.021	0.004	0.017	0.005	0.015	0.006	0.025	0.008	0.021	0.002	0.008	0.002	0.007
Flu	0.001	0.004	0.001	0.003	0.000	0.004	0.001	0.003	0.000	0.003	0.001	0.002	0.000	0.002	0.001	0.002
Phe	0.040	0.095	0.005	0.010	0.036	0.086	0.004	0.009	0.028	0.067	0.003	0.007	0.019	0.046	0.002	0.005
Ant	0.042	0.006	0.007	0.009	0.027	0.004	0.004	0.006	0.035	0.005	0.006	0.008	0.019	0.003	0.003	0.004
Fla	0.005	0.001	0.001	0.002	0.006	0.001	0.001	0.002	0.006	0.001	0.001	0.002	0.009	0.002	0.002	0.004
Pyr	0.168	0.092	0.083	0.074	0.145	0.080	0.072	0.064	0.155	0.085	0.077	0.068	0.151	0.083	0.075	0.066
BaA	0.019	0.007	0.004	0.009	0.017	0.007	0.004	0.008	0.023	0.009	0.005	0.011	0.052	0.020	0.011	0.024
Chr	0.002	0.000	0.001	0.000	0.002	0.000	0.001	0.001	0.002	0.000	0.001	0.001	0.002	0.000	0.001	0.001
BbF	0.014	0.014	0.038	0.017	0.023	0.024	0.062	0.027	0.027	0.028	0.075	0.032	0.036	0.037	0.098	0.043
BkF	0.000	0.000	0.001	0.000	0.001	0.001	0.002	0.001	0.001	0.001	0.001	0.001	0.001	0.001	0.001	0.001
BaP	0.001	0.001	0.009	0.001	0.001	0.001	0.008	0.001	0.001	0.001	0.007	0.001	0.002	0.002	0.015	0.002
DahA	0.000	0.000	0.001	0.000	0.000	0.000	0.001	0.000	0.000	0.000	0.001	0.001	0.000	0.000	0.001	0.000
Ind	0.000	0.000	0.000	0.000	0.000	0.000	0.000	0.000	0.000	0.000	0.000	0.000	0.000	0.000	0.000	0.000
BghiP	0.000	0.000	0.000	0.000	0.000	0.000	0.000	0.000	0.000	0.000	0.000	0.000	0.000	0.000	0.000	0.000
$T^{RQ_{PMF}^{j}}$	0.319	0.286	0.202	0.193	0.293	0.279	0.227	0.200	0.306	0.265	0.230	0.200	0.312	0.238	0.252	0.198

Table S5 The contribution rate ($ILCR_i$) of the ILCR of i-th PAH for the sum of ILCR in each site.

PAHs	$ILCR_i$ of PAHs in *R. philippinarum*				$ILCR_i$ of PAHs in *M. veneriformis*			
□	S1	S2	S3	S4	S1	S2	S3	S4

Nap	0.001	0.000	0.000	0.000	0.001	0.000	0.000	0.000
Acy	0.002	0.001	0.000	0.001	0.002	0.001	0.000	0.001
Ace	0.001	0.000	0.000	0.000	0.001	0.000	0.000	0.000
Flu	0.002	0.001	0.000	0.001	0.002	0.001	0.000	0.001
Phe	0.005	0.003	0.002	0.003	0.005	0.003	0.002	0.004
Ant	0.006	0.002	0.001	0.002	0.005	0.002	0.001	0.002
Fla	0.004	0.005	0.004	0.006	0.004	0.005	0.004	0.006
Pyr	0.004	0.004	0.003	0.003	0.004	0.003	0.003	0.003
BaA	0.020	0.025	0.020	0.025	0.020	0.025	0.022	0.027
Chr	0.017	0.023	0.024	0.022	0.017	0.023	0.022	0.022
BbF	0.322	0.372	0.365	0.392	0.321	0.359	0.388	0.388
BkF	0.042	0.058	0.058	0.041	0.041	0.055	0.055	0.045
BaP	0.306	0.284	0.291	0.312	0.310	0.277	0.292	0.329
DahA	0.207	0.205	0.198	0.155	0.204	0.223	0.183	0.136
Ind	0.058	0.014	0.030	0.035	0.060	0.021	0.023	0.033
BghiP	0.005	0.002	0.004	0.002	0.004	0.002	0.005	0.003

Table S6 The contribution rate (SF_{ij}) of the i-th PAH for the j-th factor (correspond to the j-th source) of PMF, in this study, which was derived from the PMF model. The “F” represented the factor derived from PMF model.

PAHs	SF_{ij} of PAHs in *R. philippinarum*				SF_{ij} of PAHs in *M. veneriformis*			
□	F1	F2	F3	F4	F1	F2	F3	F4
Nap	0.042	0.000	0.004	0.016	0.005	0.048	0.000	0.010
Acy	0.026	0.008	0.009	0.019	0.014	0.021	0.009	0.019
Ace	0.033	0.006	0.008	0.016	0.008	0.029	0.006	0.019
Flu	0.035	0.003	0.007	0.017	0.007	0.032	0.003	0.020

Phe	0.040	0.017	0.002	0.004	0.002	0.040	0.017	0.004
Ant	0.009	0.036	0.007	0.011	0.007	0.008	0.038	0.010
Fla	0.008	0.031	0.008	0.015	0.008	0.008	0.032	0.014
Pyr	0.014	0.024	0.012	0.012	0.012	0.014	0.025	0.011
BaA	0.012	0.029	0.007	0.015	0.007	0.012	0.030	0.014
Chr	0.007	0.029	0.016	0.010	0.016	0.007	0.030	0.010
BbF	0.012	0.011	0.027	0.013	0.028	0.012	0.011	0.013
BkF	0.014	0.012	0.025	0.012	0.026	0.013	0.012	0.012
BaP	0.008	0.006	0.041	0.008	0.042	0.007	0.006	0.007
DahA	0.009	0.011	0.026	0.016	0.027	0.009	0.011	0.016
Ind	0.012	0.008	0.027	0.015	0.028	0.012	0.008	0.015
BghiP	0.014	0.016	0.024	0.008	0.025	0.013	0.016	0.008
Total	0.253	0.247	0.248	0.190	0.257	0.236	0.253	0.192

Table S7 $ILCR_{PMF}^{i}$ was the calculated value of ecological risk of PAH individuals to contribution of the j-th source in *R. philippinarum*. The total $ILCR_{PMF}^{j}$ (T $ILCR_{PMF}^{j}$) was sum of the $ILCR_{PMF}^{i}$ for 16 PAHs, which was the contribution rate of j-th source to the ecological risk. The "F" represented the pollution source.

PAHs in *R. philippinarum*	$ILCR_{PMF}^{i}$ of S1				$ILCR_{PMF}^{i}$ of S2				$ILCR_{PMF}^{i}$ of S3				$ILCR_{PMF}^{i}$ of S4			
	F1	F2	F3	F4	F1	F2	F3	F4	F1	F2	F3	F4	F1	F2	F3	F4
Nap	0.000	0.000	0.000	0.000	0.000	0.000	0.000	0.000	0.000	0.000	0.000	0.000	0.000	0.000	0.000	0.000
Acy	0.001	0.000	0.000	0.001	0.000	0.000	0.000	0.000	0.000	0.000	0.000	0.000	0.000	0.000	0.000	0.000
Ace	0.000	0.000	0.000	0.000	0.000	0.000	0.000	0.000	0.000	0.000	0.000	0.000	0.000	0.000	0.000	0.000
Flu	0.001	0.000	0.000	0.000	0.000	0.000	0.000	0.000	0.000	0.000	0.000	0.000	0.001	0.000	0.000	0.000
Phe	0.003	0.001	0.000	0.000	0.002	0.001	0.000	0.000	0.001	0.001	0.000	0.000	0.002	0.001	0.000	0.000

Ant	0.001	0.003	0.001	0.001	0.000	0.001	0.000	0.000	0.000	0.001	0.000	0.000	0.000	0.001	0.000	0.000
Fla	0.001	0.002	0.001	0.001	0.001	0.003	0.001	0.001	0.000	0.002	0.000	0.001	0.001	0.003	0.001	0.001
Pyr	0.001	0.001	0.001	0.001	0.001	0.001	0.001	0.001	0.001	0.001	0.001	0.001	0.001	0.001	0.001	0.001
BaA	0.004	0.010	0.002	0.005	0.005	0.012	0.003	0.006	0.004	0.010	0.002	0.005	0.005	0.012	0.003	0.006
Chr	0.002	0.008	0.004	0.003	0.003	0.011	0.006	0.004	0.003	0.011	0.006	0.004	0.003	0.010	0.006	0.003
BbF	0.062	0.054	0.138	0.067	0.072	0.063	0.160	0.078	0.071	0.061	0.157	0.076	0.076	0.066	0.168	0.082
BkF	0.009	0.008	0.017	0.008	0.013	0.011	0.023	0.011	0.013	0.011	0.023	0.011	0.009	0.008	0.016	0.008
BaP	0.037	0.031	0.201	0.037	0.035	0.029	0.186	0.034	0.036	0.029	0.191	0.035	0.038	0.032	0.205	0.038
DahA	0.031	0.036	0.086	0.053	0.031	0.036	0.086	0.053	0.030	0.035	0.082	0.051	0.023	0.027	0.065	0.040
Ind	0.011	0.007	0.025	0.014	0.003	0.002	0.006	0.003	0.006	0.004	0.013	0.007	0.007	0.004	0.015	0.008
BghiP	0.001	0.001	0.002	0.001	0.000	0.000	0.001	0.000	0.001	0.001	0.001	0.000	0.001	0.001	0.001	0.000
T$ILCR_{PMF}^{j}$	0.166	0.164	0.478	0.192	0.166	0.169	0.472	0.193	0.165	0.166	0.477	0.192	0.166	0.165	0.480	0.189

Table S8 $ILCR_{PMF}^{i}$ was the calculated value of ecological risk of PAH individuals to contribution of the j-th source in *M. veneriformis*. The total $ILCR_{PMF}^{j}$ (T $ILCR_{PMF}^{j}$) was sum of the $ILCR_{PMF}^{i}$ for 16 PAHs, which was the contribution rate of j-th source to the ecological risk. The "F" represented the pollution source.

PAHs in *M. veneriformis*	$ILCR_{PMF}^{i}$ of S1				$ILCR_{PMF}^{i}$ of S2				$ILCR_{PMF}^{i}$ of S3				$ILCR_{PMF}^{i}$ of S4			
	F1	F2	F3	F4	F1	F2	F3	F4	F1	F2	F3	F4	F1	F2	F3	F4
Nap	0.000	0.000	0.000	0.000	0.000	0.000	0.000	0.000	0.000	0.000	0.000	0.000	0.000	0.000	0.000	0.000
Acy	0.000	0.001	0.000	0.001	0.000	0.000	0.000	0.000	0.000	0.000	0.000	0.000	0.000	0.000	0.000	0.000
Ace	0.000	0.000	0.000	0.000	0.000	0.000	0.000	0.000	0.000	0.000	0.000	0.000	0.000	0.000	0.000	0.000
Flu	0.000	0.001	0.000	0.001	0.000	0.000	0.000	0.000	0.000	0.000	0.000	0.000	0.000	0.001	0.000	0.000
Phe	0.000	0.003	0.001	0.000	0.000	0.002	0.001	0.000	0.000	0.001	0.001	0.000	0.000	0.002	0.001	0.000

Ant	0.001	0.001	0.003	0.001	0.000	0.000	0.001	0.000	0.000	0.000	0.001	0.000	0.000	0.000	0.001	0.000
Fla	0.001	0.001	0.002	0.001	0.001	0.001	0.002	0.001	0.001	0.000	0.002	0.001	0.001	0.001	0.003	0.001
Pyr	0.001	0.001	0.001	0.001	0.001	0.001	0.001	0.001	0.001	0.001	0.001	0.001	0.001	0.001	0.001	0.000
BaA	0.002	0.004	0.009	0.004	0.003	0.005	0.012	0.006	0.002	0.004	0.010	0.005	0.003	0.005	0.013	0.006
Chr	0.004	0.002	0.008	0.003	0.006	0.003	0.011	0.003	0.006	0.002	0.010	0.003	0.006	0.002	0.011	0.003
BbF	0.143	0.059	0.054	0.066	0.160	0.066	0.060	0.073	0.172	0.071	0.065	0.079	0.172	0.071	0.065	0.079
BkF	0.017	0.009	0.008	0.008	0.023	0.011	0.011	0.010	0.022	0.011	0.011	0.010	0.019	0.009	0.009	0.008
BaP	0.208	0.035	0.031	0.036	0.186	0.031	0.028	0.032	0.196	0.033	0.030	0.034	0.220	0.037	0.033	0.038
DahA	0.088	0.029	0.036	0.052	0.097	0.031	0.039	0.057	0.079	0.026	0.032	0.046	0.059	0.019	0.024	0.035
Ind	0.027	0.012	0.007	0.014	0.009	0.004	0.003	0.005	0.011	0.005	0.003	0.006	0.015	0.006	0.004	0.008
BghiP	0.002	0.001	0.001	0.001	0.001	0.000	0.000	0.000	0.002	0.001	0.001	0.001	0.001	0.001	0.001	0.000
$T^{ILCR_{PMF}^{j}}$	0.494	0.156	0.163	0.187	0.485	0.156	0.170	0.189	0.491	0.156	0.166	0.186	0.497	0.156	0.166	0.181

Table S9 PAH concentrations in seawater, sediment, and shellfish of other coastal areas worldwide.

Ambient media	Region of coastal areas (and species)	Total concentration of 16 PAHs
Seawater	The Bohai Bay, China	48.0 to 607 ng/L
	The Pearl River Estuary, China	25.99 to 522.26 ng/L
	The Hainan Island, China	273.79 to 407.82 ng/L
	The Kongsfjorden, Arctic	33.4 to 79.8 ng/L
	The Suez Bay, Red Sea	0.502 to 43.540 ng/L
	The Chabahar Bay, Oman Sea	0.04 to 59.6 ng/L
Sediment	The Yangtze River Estuary, China	84.6 to 620 ng/g d.w.
	The Mahandi River Estuary, India	13.1 to 685.4 ng/g d.w.
	The Estuary of St. Lawrence, Canada	71 to 5672 ng/g d.w.
	The Yellow River Estuary, China	10.8 to 252 ng/g d.w.
	The Goiana Estuary, Brazil	0.006 to 156 ng/g d.w.
	The Paranagua Estuarine System, South Atlantic	0 to 125.6 ng/g d.w.
Shellfish	The Arcachon Bay, France (mussels *Mytilus edulis*)	110 to 1450 ng/g d.w.
	The Hainan Island, China (pearl oyster *Pinctada martensii*)	597.1 to 2332 ng/g d.w.
	The Jakarta Bay, Indonesia (green mussels *Perna viridis*)	591 to 997 ng/g d.w.
	Coastal environment of Valparaiso, Chile (mussels *Perumytilus purpuratus*)	27.3 to 253.1 ng/g d.w.
	Plentzia in Bay of Biscay, North Atlantic (mussels *Mytilus galloprovincialis*)	207 to 483 ng/g d.w.
	The Levrier Bay, south Atlantic coast (mussels *Perna perna*)	238 to 253 ng/g d.w.

Table S10 Risk classification of PAH congeners and ΣPAHs based on RQ.

Individual PAH			ΣPAHs		
RQ_{NCs}	RQ_{MPCs}	Level	$RQ_{\Sigma PAHs(NCs)}$	$RQ_{\Sigma PAHs(MPCs)}$	Level
0	-	Risk-free	<1	-	Risk-free
≥1	<1	Moderate-risk	≥1; <800	<1	Low-risk
			≥800	<1	Moderate-risk 1
			<800	≥1	Moderate-risk 2
-	≥1	High-risk	≥800	≥1	High-risk

*$RQ_{(NCs)}$: risk quotient of individual PAH negligible concentrations; $RQ_{(MPCs)}$: risk quotient of individual PAH maximum permissible concentrations (MPCs); $RQ_{\Sigma PAHs\,(NCs)}$: risk quotient of PAHs negligible concentrations; $RQ_{\Sigma PAHs\ (MPCs)}$: risk quotient of PAHs maximum permissible concentrations (MPCs).

Table S11 Spearman correlation analysis between total PAH concentrations in sediment (-S), soft tissue of *R. philippinarum* (-*R*) and various biomarkers.

n=36	Individual

	CI	CIL	ST	GI	HSI				
R-S	-0.164	-0.062	0.405	-0.207	-0.095				
Sig.-S	0.339	0.722	0.014	0.226	0.580				
R-*R*	-0.089	0.028	0.370	-0.349	-0.166				
Sig.-*R*	0.605	0.873	0.026	0.037	0.335				
					Gill				
	EROD	GST	T-AOC	SOD	CAT	GPx	GSH	LPO	DNAD
R-S	0.122	0.208	-0.056	0.211	0.366	0.619	0.222	-0.271	0.058
Sig.-S	0.479	0.224	0.744	0.217	0.028	<0.001	0.192	0.111	0.735
R-*R*	0.539	0.514	-0.325	0.564	0.456	0.69	0.063	0.108	0.012
Sig.-*R*	<0.001	0.001	0.053	<0.001	0.005	<0.001	0.715	0.529	0.945
	PCC	AChE	HSP22-2	HSP40A	HSP60	HSP70	HSP90	P-gp	AhR
R-S	0.227	-0.284	0.005	-0.183	0.019	0.202	0.116	0.425	-0.13
Sig.-S	0.184	0.093	0.979	0.286	0.914	0.237	0.500	0.010	0.449
R-*R*	0.318	-0.49	0.056	-0.202	-0.079	-0.013	-0.136	0.047	-0.241
Sig.-*R*	0.059	0.002	0.747	0.237	0.647	0.939	0.431	0.784	0.157
	CYP1A1	GST-pi	GST-mu	ABCC1	MnSOD	CAT-g	GPx-g		
R-S	-0.043	0.182	0.332	0.167	0.081	-0.048	0.136		
Sig.-S	0.802	0.288	0.048	0.329	0.637	0.781	0.431		
R-*R*	-0.189	-0.096	0.034	-0.115	-0.005	-0.236	0.081		
Sig.-*R*	0.270	0.577	0.844	0.503	0.979	0.165	0.637		
					Digestive gland				
	EROD	GST	T-AOC	SOD	CAT	GPx	GSH	LPO	DNAD
R-S	0.380	0.134	-0.004	0.364	0.577	0.561	-0.214	0.550	0.047
Sig.-S	0.022	0.435	0.982	0.029	<0.001	<0.001	0.21	<0.001	0.784
R-*R*	0.548	0.352	-0.016	0.503	0.710	0.749	-0.025	0.765	0.162
Sig.-*R*	<0.001	0.035	0.924	0.002	<0.001	<0.001	0.883	<0.001	0.345
	PCC	AChE	HSP22-2	HSP40A	HSP60	HSP70	HSP90	P-gp	AhR
R-S	-0.232	-0.408	-0.587	-0.414	-0.347	-0.365	-0.092	-0.222	-0.388
Sig.-S	0.174	0.014	<0.001	0.012	0.038	0.029	0.593	0.193	0.019
R-*R*	-0.229	-0.658	-0.334	-0.298	-0.299	-0.14	-0.146	-0.225	-0.123
Sig.-*R*	0.179	<0.001	0.047	0.077	0.076	0.415	0.394	0.186	0.474
	CYP1A1	GST-pi	GST-mu	ABCC1	MnSOD	CAT-g	GPx-g		
R-S	-0.232	-0.163	-0.059	-0.214	-0.003	-0.025	0.309		
Sig.-S	0.174	0.341	0.733	0.211	0.986	0.886	0.067		
R-*R*	-0.014	-0.204	-0.167	-0.098	-0.011	-0.081	0.054		
Sig.-*R*	0.936	0.232	0.332	0.571	0.950	0.637	0.753		
					Hemocyte & plasma				
	THC	PA	LMS	AA	BA				
R-S	-0.038	-0.115	-0.246	-0.040	-0.151				
Sig.-S	0.828	0.506	0.149	0.815	0.378				
R-*R*	-0.004	0.041	-0.575	-0.145	-0.222				
Sig.-*R*	0.980	0.810	<0.001	0.398	0.193				

*DNAD: DNA damage, CAT-g and GPx-g: mRNA expression of CAT and GPx gene, PA: phagocytic activity, AA: antibacterial activity, BA: bacteriolytic activity.

Table S12 Spearman correlation analysis between total PAH concentrations in sediment (-S), soft tissue of *M. veneriformis* (-*M*) and various biomarkers.

n=36					Individual				
	CI	CIL	ST	GI	HSI				
R-S	-0.342	-0.212	0.358	-0.116	-0.212				
Sig.-S	0.041	0.214	0.032	0.501	0.215				
R-*M*	-0.161	-0.063	0.270	-0.130	-0.227				
Sig.-*M*	0.348	0.716	0.111	0.451	0.184				
					Gill				
	EROD	GST	T-AOC	SOD	CAT	GPx	GSH	LPO	DNAD
R-S	0.366	0.338	0.355	0.354	0.721	0.703	0.069	-0.211	0.057
Sig.-S	0.028	0.043	0.034	0.034	<0.001	<0.001	0.687	0.216	0.743
R-*M*	0.516	0.607	0.115	0.567	0.445	0.563	-0.207	0.209	0.083
Sig.-*M*	0.001	<0.001	0.504	<0.001	0.007	<0.001	0.225	0.222	0.630
	PCC	AChE							
R-S	0.010	-0.259							
Sig.-S	0.955	0.127							
R-*M*	0.227	-0.383							
Sig.-*M*	0.183	0.021							
					Digestive gland				
	EROD	GST	T-AOC	SOD	CAT	GPx	GSH	LPO	DNAD
R-S	0.309	0.056	-0.014	0.091	0.208	0.344	-0.014	0.438	0.310
Sig.-S	0.067	0.744	0.936	0.599	0.224	0.040	0.936	0.008	0.066
R-*M*	0.787	0.457	-0.060	0.351	0.646	0.700	0.099	0.632	0.403
Sig.-*M*	<0.001	0.005	0.726	0.036	<0.001	<0.001	0.567	<0.001	0.015
	PCC	AChE							
R-S	-0.102	-0.105							
Sig.-S	0.555	0.542							
R-*M*	0.07	-0.546							
Sig.-*M*	0.686	<0.001							
					Hemocyte & plasma				
	THC	PA	LMS	AA	BA				
R-S	0.181	0.108	-0.078	-0.219	0.153				
Sig.-S	0.292	0.531	0.651	0.199	0.373				
R-*M*	-0.120	0.058	-0.630	0.048	0.128				
Sig.-*M*	0.485	0.737	<0.001	0.779	0.457				

Table S13 Model parameters of positive matrix factorization (PMF).

Parameter	Seawater				Sediment			
	3 factors	4 factors	5 factors	6 factors	3 factors	4 factors	5 factors	6 factors
Q (Robust)	2233.8	1790.9	1400.9	1076.4	2392.8	1667.8	1146.3	854.7

Q (True)	2813.5	1991.8	1911.5	1198.5	3135.3	1891.1	1429.5	1067.3
QR/QT	79.40%	89.91%	73.29%	89.81%	76.32%	88.19%	80.19%	80.08%
	Ruditapes philippinarum				*Mactra veneriformis*			
	3 factors	4 factors	5 factors	6 factors	3 factors	4 factors	5 factors	6 factors
Q (Robust)	9080.6	5970.6	4393.9	2910.2	11305.8	8129.5	5623.8	3730.0
Q (True)	13092.6	7365.8	6569.8	5088.1	17804.3	9724.7	8035.6	5893.2
QR/QT	69.36%	81.06%	66.88%	57.20%	63.50%	83.60%	69.99%	63.29%

Table S14 Toxicity equivalence factors (TEFs) for the 16 PAHs.

PAH	Nap	Acy	Ace	Flu	Phe	Ant	Fla	Pyr
TEF	0.001	0.001	0.001	0.001	0.001	0.01	0.001	0.001
PAH	BaA	Chr	BbF	BkF	BaP	DahA	Ind	BghiP
TEF	0.1	0.01	0.1	0.1	1	1	0.1	0.01

Table S15 The MS parameters, matrix spike recovery and MDLs for the PAH analytes in seawater.

Analyte	Retention time (min)	m/z for SIM	Matrix spike recovery (%)	MDLs (ng/L)
Acy	8.146	152, 151, 153	74±11	0.020
Ace-d_{10}	8.443	164, 162, 160	99±10	surrogate
Ace	8.571	153, 154, 152	73±7	0.021
Flu	9.686	166, 165, 167	82±13	0.028
TCMX	11.174	207, 209, 244	internal standard	-
Phe-d_{10}	11.761	188, 184	102±8	surrogate
Phe	11.923	178, 179	82±11	0.038
Ant	12.024	178, 179, 176	82±10	0.021
Fla	14.370	202, 101, 100	93±6	0.173
Pyr	14.874	202, 200, 203	101±11	0.138
BaA	17.428	228, 226	111±10	0.043
Chr-d_{12}	17.487	240, 236	105±10	surrogate
Chr	17.518	228, 229, 226	102±10	0.049
BbF	19.584	252, 253, 125	108±10	0.196
BkF	19.632	252, 253, 250	109±9	0.080
BaP	20.390	252, 253, 250	96±9	0.100
perylene-d_{12}	20.549	264, 260	99±5	surrogate
BghiP	24.665	276, 274, 138	94±7	0.029

Table S16 The MS parameters, matrix spike recovery and MDLs for the PAH analytes in sediment.

Analyte	Retention time (min)	m/z for SIM	Matrix spike recovery (%)	MDLs (ng/g)
2-fluorobiphenyl	7.190	172, 171, 170	92±12	surrogate
Acy	7.984	152, 151, 153	88±5	0.039
Ace-d_{10}	8.226	162, 167, 160, 163	internal standard	-
Ace	8.302	154, 153, 152	79±6	0.032
Flu	9.222	166, 165, 167	89±7	0.029

Phe-d_{10}	12.143	188, 189, 160, 94	internal standard	-
Phe	12.301	178, 179, 176	111±13	0.108
Ant	12.477	178, 179, 176	95±5	0.042
Fla	16.497	202, 200, 203, 101, 100	103±9	0.176
Pyr	17.114	202, 200, 203, 101, 100	102±9	0.106
P-terphenyl-d_{14}	17.949	244, 245, 243	102±10	surrogate
BaA	20.451	228, 226, 229, 114, 113	106±8	0.068
Chr-d_{12}	20.561	240, 236, 238, 241	internal standard	-
Chr	20.638	228, 226, 229, 114, 113	85±9	0.126
BbF	23.195	252, 253, 250, 251	85±8	0.137
BkF	23.273	252, 253, 250, 251	94±7	0.018
BaP	23.950	252, 253, 250, 251	97±11	0.125
perylene-d_{12}	24.114	264, 260, 265, 263	internal standard	-
Ind	27.253	276, 277, 275, 274	92±9	0.022
DahA	27.417	278, 276, 279, 138	88±6	0.047
BghiP	28.131	276, 275, 274, 138	103±7	0.019

Table S17 The MS parameters, matrix spike recovery and MDLs for the PAH analytes in clam soft tissue.

Analyte	Retention time (min)	m/z for SIM	Matrix spike recovery (%)	MDLs (ng/g)
Nap	3.565	128, 64, 102	95±10	0.036
Acy	5.493	152, 63, 76	82±9	0.703
Ace	5.681	153, 154, 76	81±8	0.177
Flu	6.337	166, 165, 82	78±10	0.530
Phe	7.704	178, 89, 152	94±15	1.130
Ant	7.803	178, 89, 152	96±11	0.054
Fla	9.957	202, 101, 200	95±10	1.186
Pyr	10.561	202, 101, 200	107±10	0.904
BaA	14.119	228, 114, 226	108±9	0.084
Chr	14.407	228, 114, 226	90±11	0.312
BbF	18.173	252, 126, 250	98±10	0.213
BkF	18.354	252, 126, 250	96±8	0.365
BaP	19.448	252, 126, 250	101±9	0.336
Ind	23.405	276, 138, 277	98±12	0.034
DahA	23.615	278, 138, 276	91±11	0.029
BghiP	24.256	276, 138, 277	98±8	0.077

Table S18 Primer sequences of clam *R. philippinarum* used in the present study listed.

Primer name	Accession no.	Primer sequences (5'→3')
HSP22-2-qF	GQ384408.1	CCCACTTGTCGGAGGATGGA
HSP22-2-qR		TCTCCAGGTGCTCGATTGGT
HSP40A-qF	GQ384397.1	ACATTCCCAGAGGAAGGCGA
HSP40A-qR		GGTTGACACCCTCGCGTCTA
HSP60-qF	KT987978.1	TTGCTGAAGATGTGGACGGTGAAG

HSP60-qR		CCTCCACTAGCAACTGCCATGTC
HSP70-qF	KJ569079.1	AAGACGCTGTTGTCACGGTTCC
HSP70-qR		GGCGGCAGCAGTTGGTTCG
HSP90-qF	KJ569080.1	TCCAGGCGGAAATTGCTCAG
HSP90-qR		CCCACTGTCCAGCTTGGATG
P-gp/ABCB1-qF	FJ612109	CCCGAGGAAGGTGTTGTGTA
P-gp/ABCB1-qR		TGGTGTCATAGCCCTCAGGT
AhR-qF	FJ516743.2	ATGCATGGTCAGCCAAACAG
AhR-qR		TCCCTTGAAGGAAGGTCCATT
CYP1A1-qF	ADP24121	AGGACCGAGGTCATGTTTAG
CYP1A1-qR		GGATTTAGAGTTGTCGCCAG
GST-pi-qF	FJ516741.2	TGCCATTTGGTCAATCGCCT
GST-pi-qR		ACGGGCCTCTAATGTCCTCC
GST-mu-qF	JN593116.2	TGAGCAGAGAGGCATGGACT
GST-mu-qR		GCGATATGCTTCAGAAGTGCG
ABCC1-qF	-	TGGCCGTTCTGGTGAATATCTTACAC
ABCC1-qR		CTTGCACTTGAGAAGCATCTGTTGAC
Mn-SOD-qF	JN593115.1	AAGGACATGTTGACACAGGC
Mn-SOD-qR		AAAGCCTGTTGTTGGTTGCAG
CAT-qF	EF520699.1	GCACACCTGATGGCTACAGAC
CAT-qR		TCACCAGCCTTATCTGCCATA
GPx-qF	HQ891002.1	TTGATTGTCAACGTGGCTACC
GPx-qR		ATTCCAAGCTGGTTCTTGCAT
EF1A-qF	PRJNA479743	TGTAGAGAGGAAGGAAGGAAATGC
EF1A-qR		GTCTTGCTGGTGGAAGGATGG
RPS23-qF	PRJNA479743	GGTGTTGGTTGCTGGTTTTGG
RPS23-qR		TTGGTCGTTCCTTCTTTCCTCTG

Table S19 Biomarker pollution index given for each biomarker response according to their rank in a scale related to the discriminatory factor.

	Discriminatory factor (DF)				
	1	2	3	4	5
Biomarker pollution index (BPI)	4	10			
	3	6	12		
	2	4	7	12	
	1	2	4	8	14

Supplementary Figures

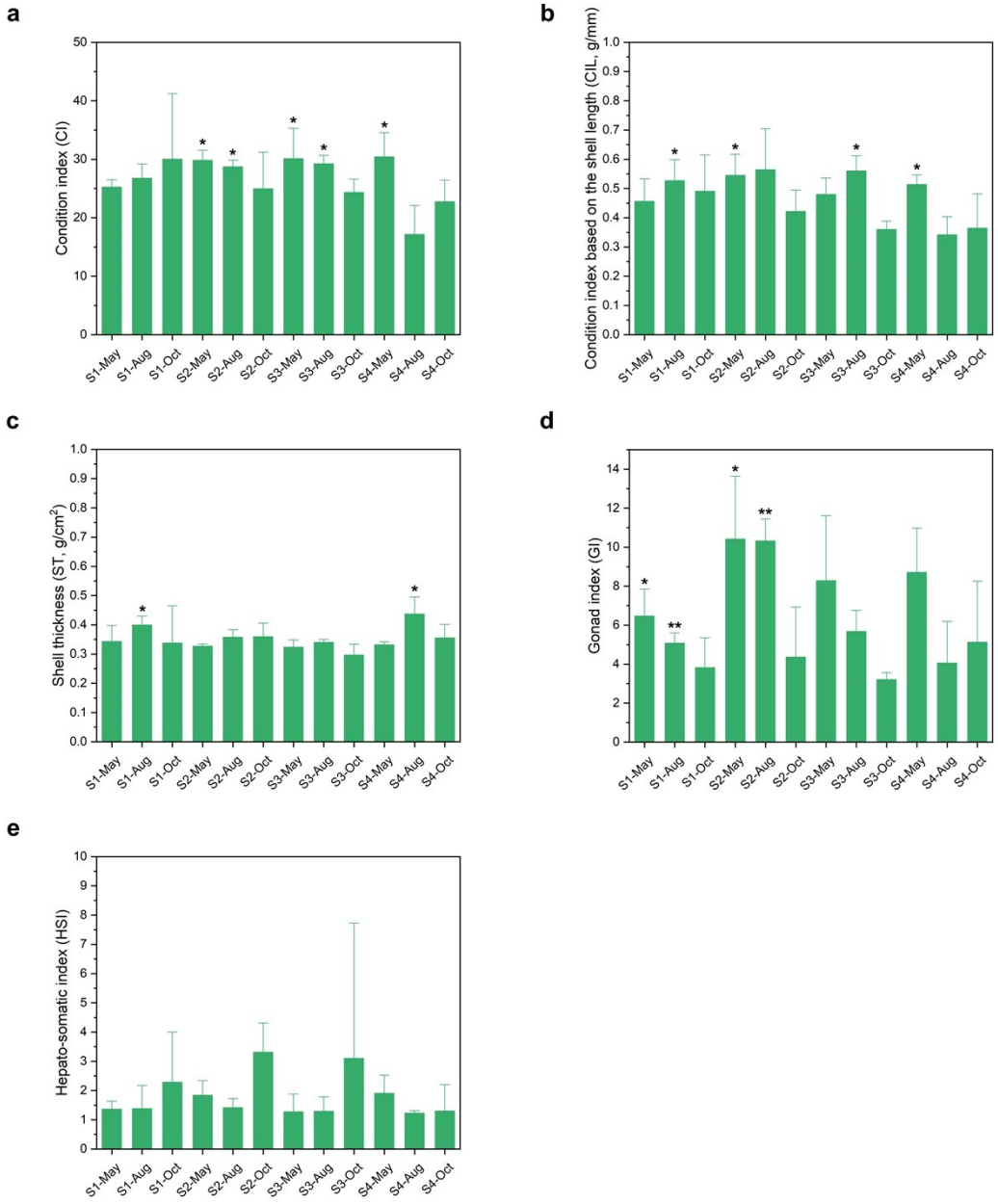

Fig. S1. The biomarkers reflecting individual growth: condition index-CI (a), condition index based on the shell length-CIL (b), shell thickness-ST (c), gonad index-GI (d), and hepato-somatic index-HSI (e) of *Ruditapes philippinarum* collected at the 4 sites in 2021. Values are presented in bar chart (n = 3). Asterisk denotes significant differences between the minimum and the other using one-way ANOVA followed by Duncan's test (*$P < 0.05$, **$P < 0.01$).

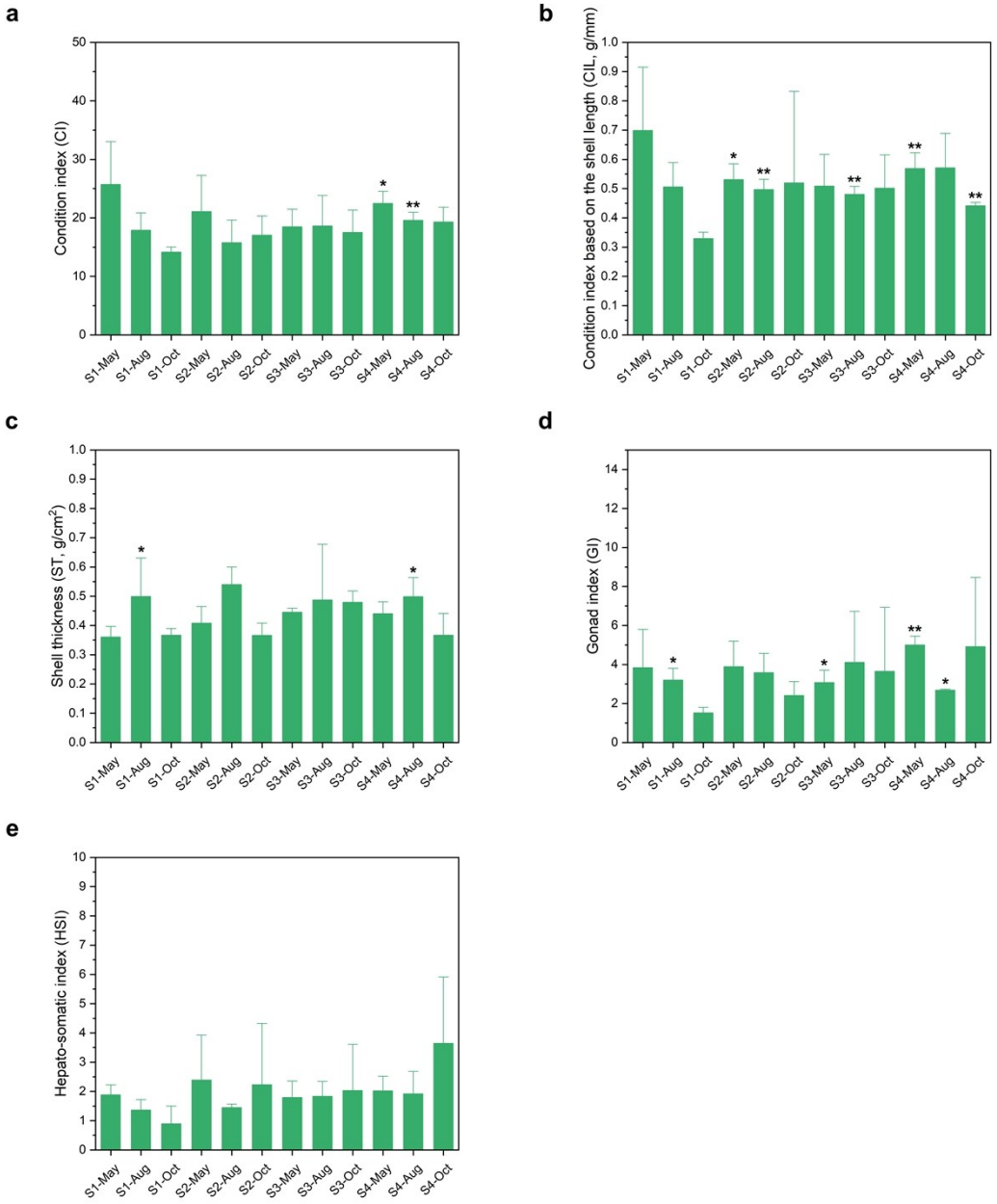

Fig. S2. The biomarkers reflecting individual growth: condition index-CI (a), condition index based on the shell length-CIL (b), shell thickness-ST (c), gonad index-GI (d), and hepato-somatic index-HSI (e) of *Mactra veneriformis* collected at the 4 sites in 2021. Values are presented in bar chart (n = 3). Asterisk denotes significant differences between the minimum and the other using one-way ANOVA followed by Duncan's test (**P* < 0.05, ***P* < 0.01).

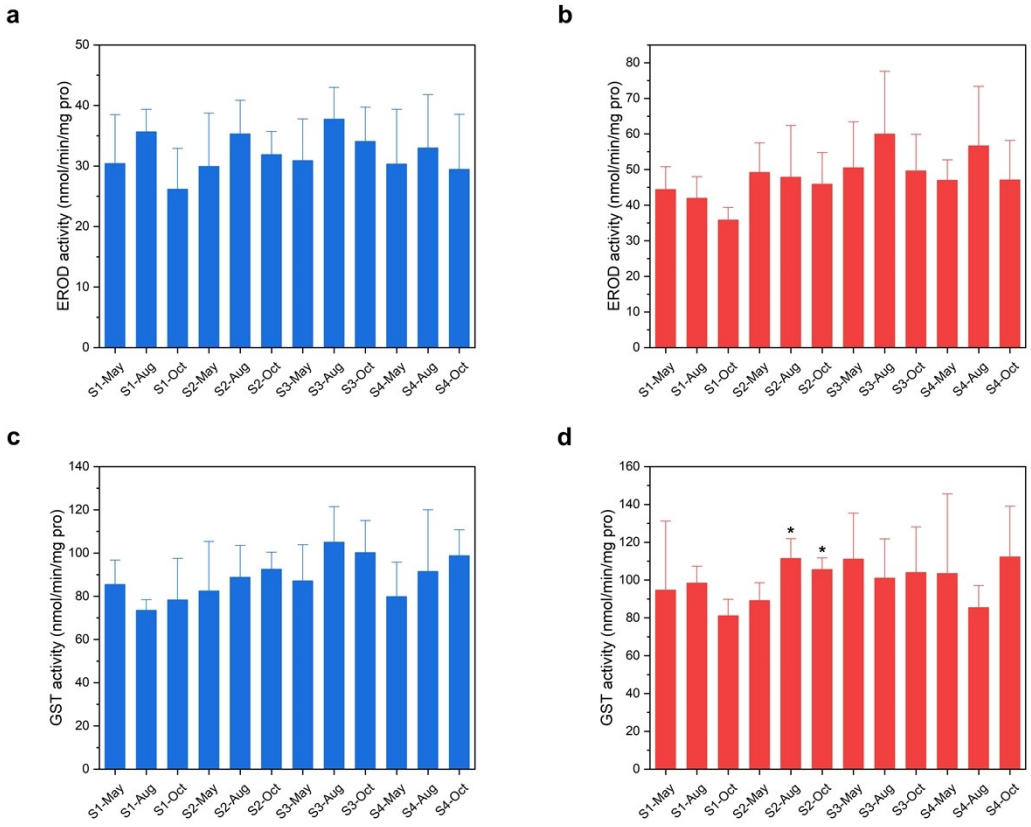

Fig. S3. The biological responses of detoxification enzyme activities: ethoxyresorufin-O-deethylase (EROD) (a, b) and glutathione S-transferase (GST) (c, d) in gills (blue) and digestive glands (red) of *Ruditapes philippinarum* collected at the 4 sites in 2021. Values are presented in bar chart (n = 3). Asterisk denotes significant differences between the minimum and the other using one-way ANOVA followed by Duncan's test (*$P < 0.05$, **$P < 0.01$).

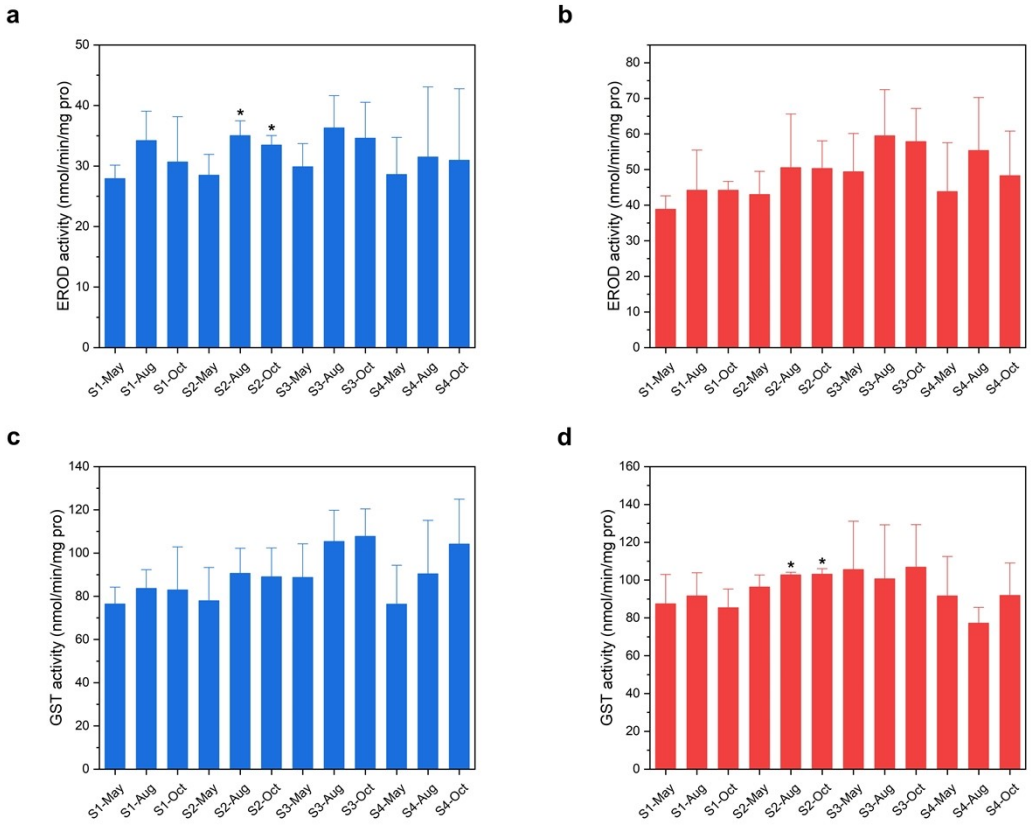

Fig. S4. The biological responses of detoxification enzyme activities: ethoxyresorufin-O-deethylase (EROD) (a, b) and glutathione S-transferase (GST) (c, d) in gills (blue) and digestive glands (red) of *Mactra veneriformis* collected at the 4 sites in 2021. Values are presented in bar chart (n = 3). Asterisk denotes significant differences between the minimum and the other using one-way ANOVA followed by Duncan's test (*$P < 0.05$, **$P < 0.01$).

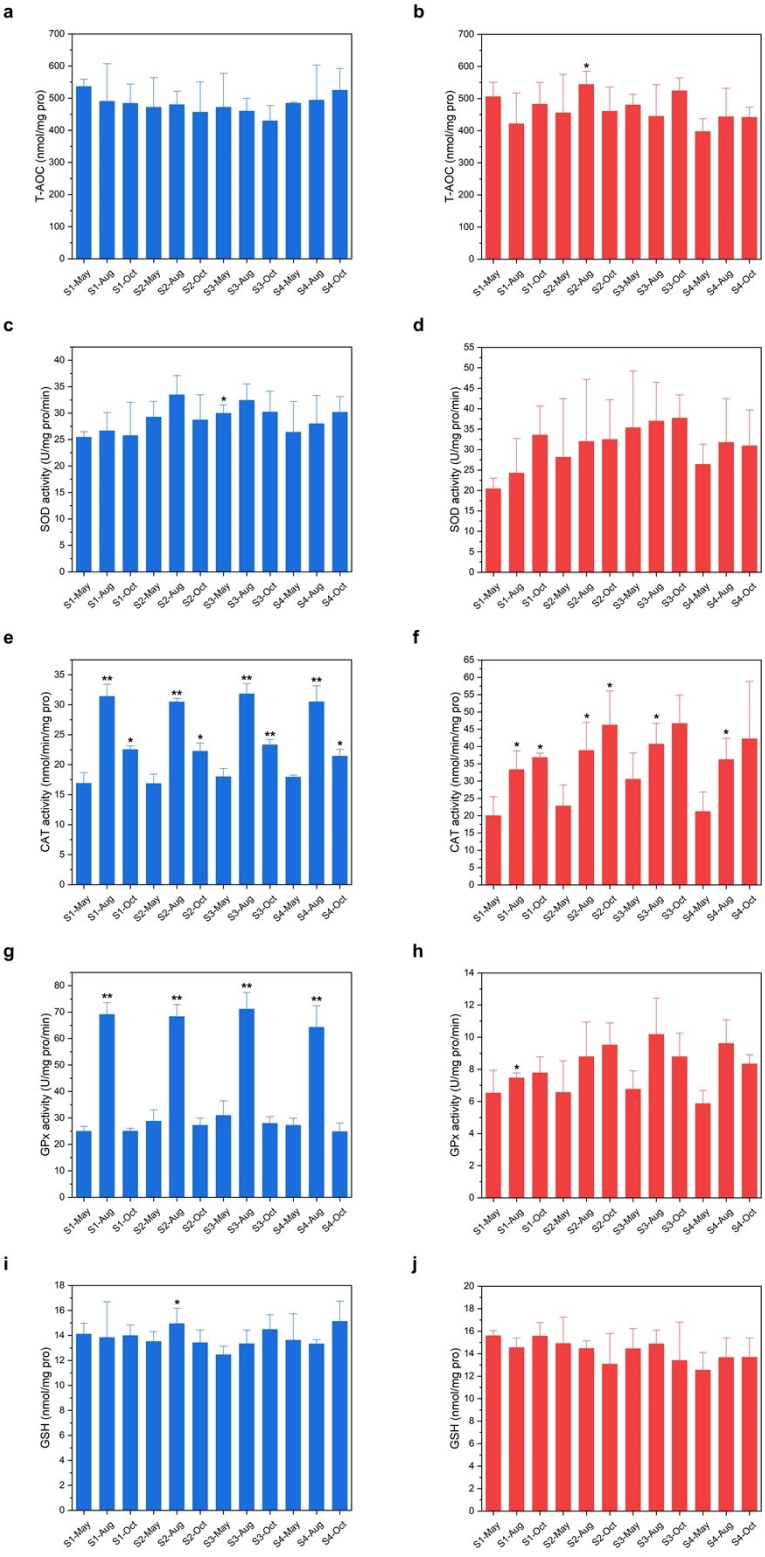

Fig. S5. The biological responses of antioxidant indictors: total antioxidant capacity (T-AOC) (a, b), superoxide dismutase (SOD) (c, d), catalase (CAT) (e, f), glutathione peroxidase (GPx) (g, h), and glutathione (GSH) (i, j) in gills (blue) and digestive glands (red) of *Ruditapes philippinarum* collected at the 4 sites in 2021. Values are presented in bar chart (n = 3). Asterisk denotes significant differences between the minimum and the other using one-way ANOVA followed by Duncan's test (*$P < 0.05$, **$P < 0.01$).

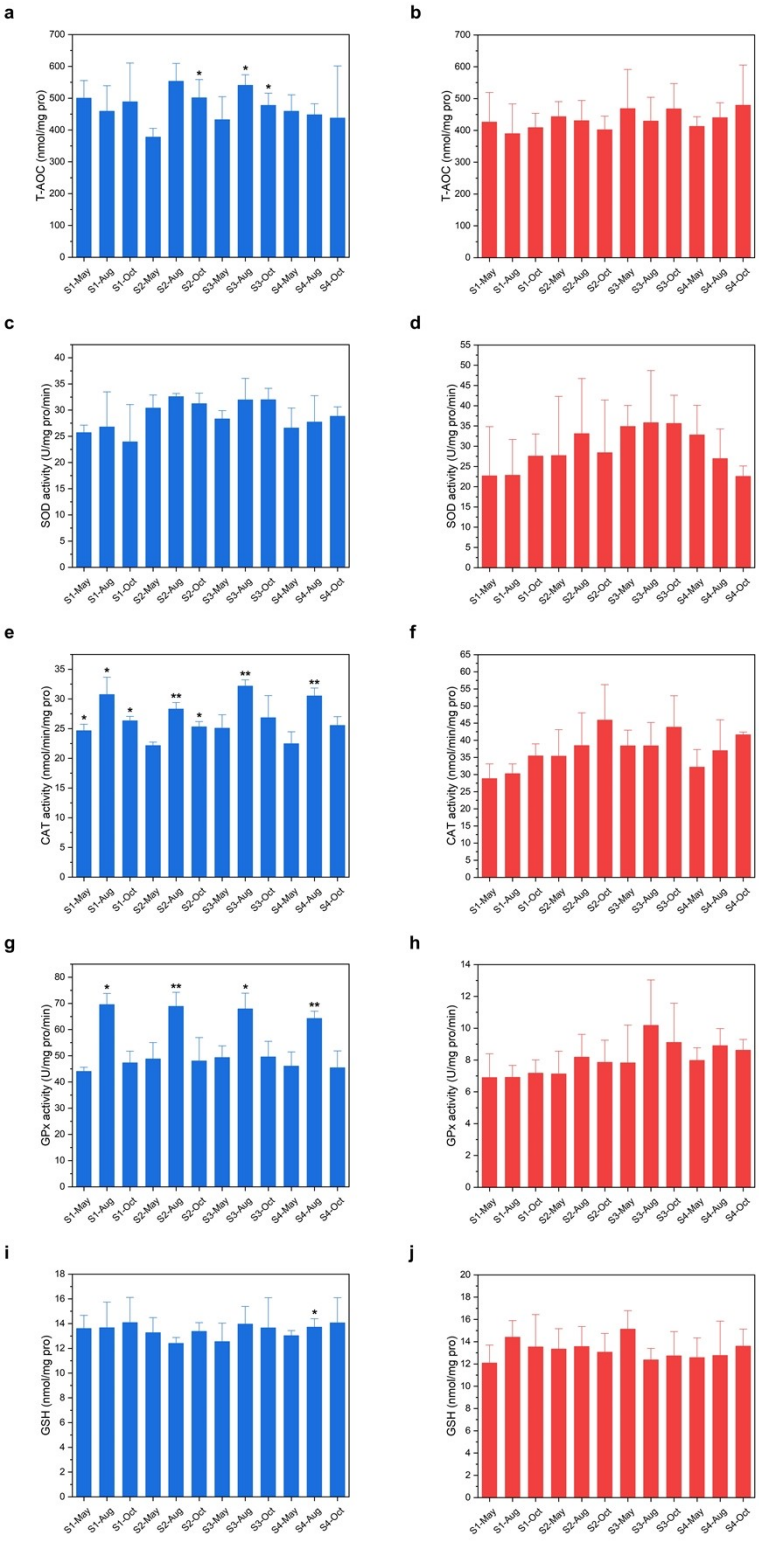

Fig. S6. The biological responses of antioxidant indictors: total antioxidant capacity (T-AOC) (a, b), superoxide dismutase (SOD) (c, d), catalase (CAT) (e, f), glutathione peroxidase (GPx) (g, h), and glutathione (GSH) (i, j) in gills (blue) and digestive glands (red) of *Mactra veneriformis* collected at the 4 sites in 2021. Values are presented in bar chart (n = 3). Asterisk denotes significant differences between the minimum and the other using one-way ANOVA followed by Duncan's test (*$P < 0.05$, **$P < 0.01$).

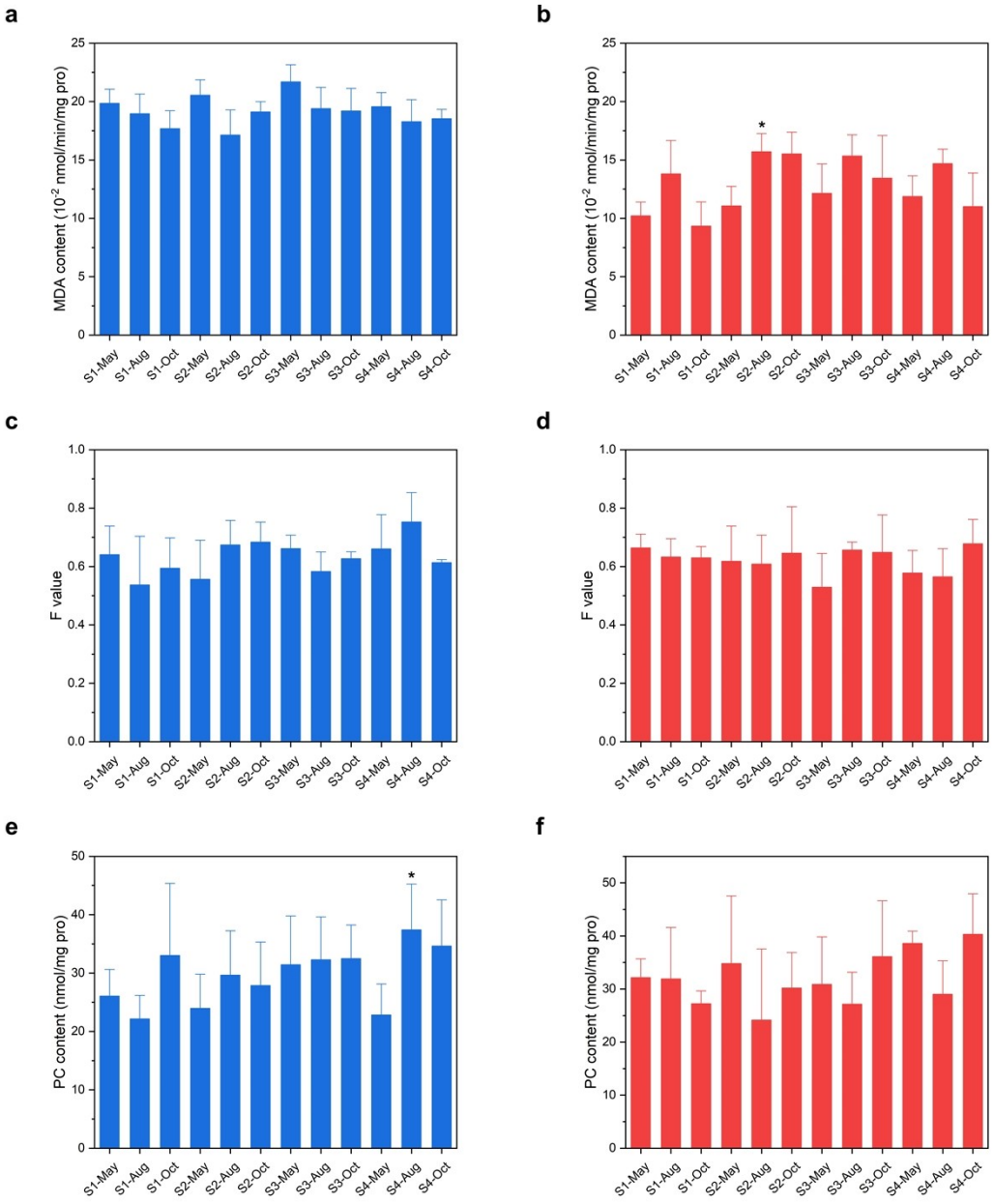

Fig. S7. The biological responses of biomacromolecular damage indictors - lipid peroxidation (LPO) expressed by malondialdehyde (MDA) content (a, b), DNA damage expressed by F value (c, d), and protein carbonylation (PC) content (e, f) in gills (blue) and digestive glands (red) of *Ruditapes philippinarum* collected at the 4 sites in 2021. Values are presented in bar chart (n = 3). Asterisk denotes significant differences between the minimum and the other using one-way ANOVA followed by Duncan's test (*$P < 0.05$, **$P < 0.01$).

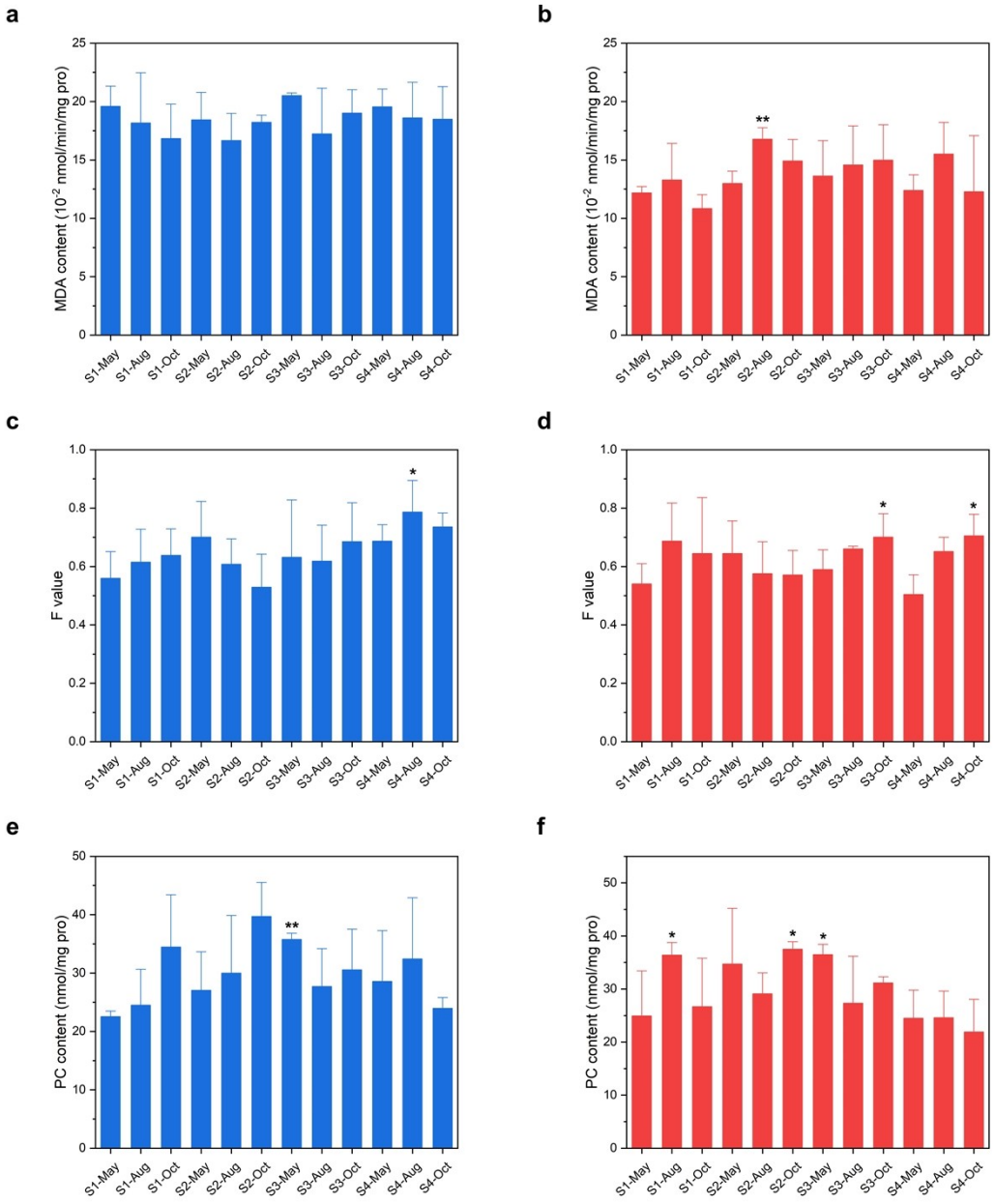

Fig. S8. The biological responses of biomacromolecular damage indictors - lipid peroxidation (LPO) expressed by malondialdehyde (MDA) content (a, b), DNA damage expressed by F value (c, d), and protein carbonylation (PC) content (e, f) in gills (blue) and digestive glands (red) of *Mactra veneriformis* collected at the 4 sites in 2021. Values are presented in bar chart (n = 3). Asterisk denotes significant differences between the minimum and the other using one-way ANOVA followed by Duncan's test (*$P < 0.05$, **$P < 0.01$).

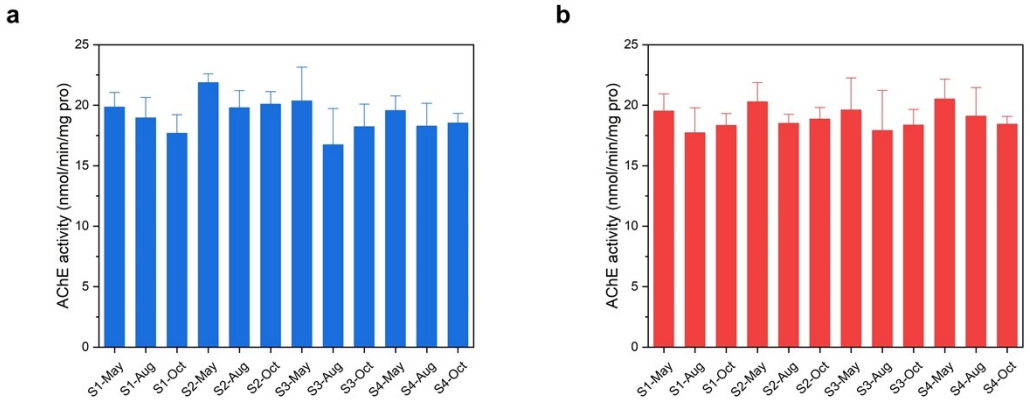

Fig. S9. The biological responses of neurotoxicity indicator: acetylcholinesterase (AChE) (a, b) in gills (blue) and digestive glands (red) of *Ruditapes philippinarum* collected at the 4 sites in 2021. Values are presented in bar chart (n = 3). Asterisk denotes significant differences between the minimum and the other using one-way ANOVA followed by Duncan's test (*$P < 0.05$, **$P < 0.01$).

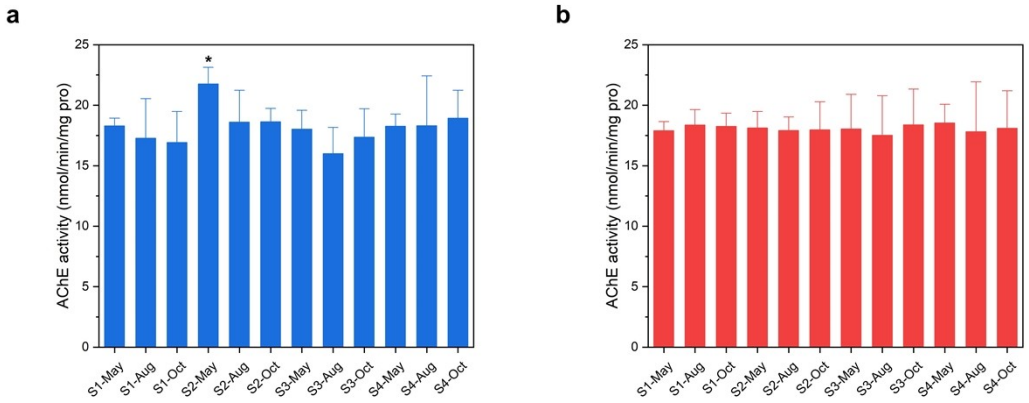

Fig. S10. The biological responses of neurotoxicity indicator: acetylcholinesterase (AChE) (a, b) in gills (blue) and digestive glands (red) of *Mactra veneriformis* collected at the 4 sites in 2021. Values are presented in bar chart (n = 3). Asterisk denotes significant differences between the minimum and the other using one-way ANOVA followed by Duncan's test (**P* < 0.05, ***P* < 0.01).

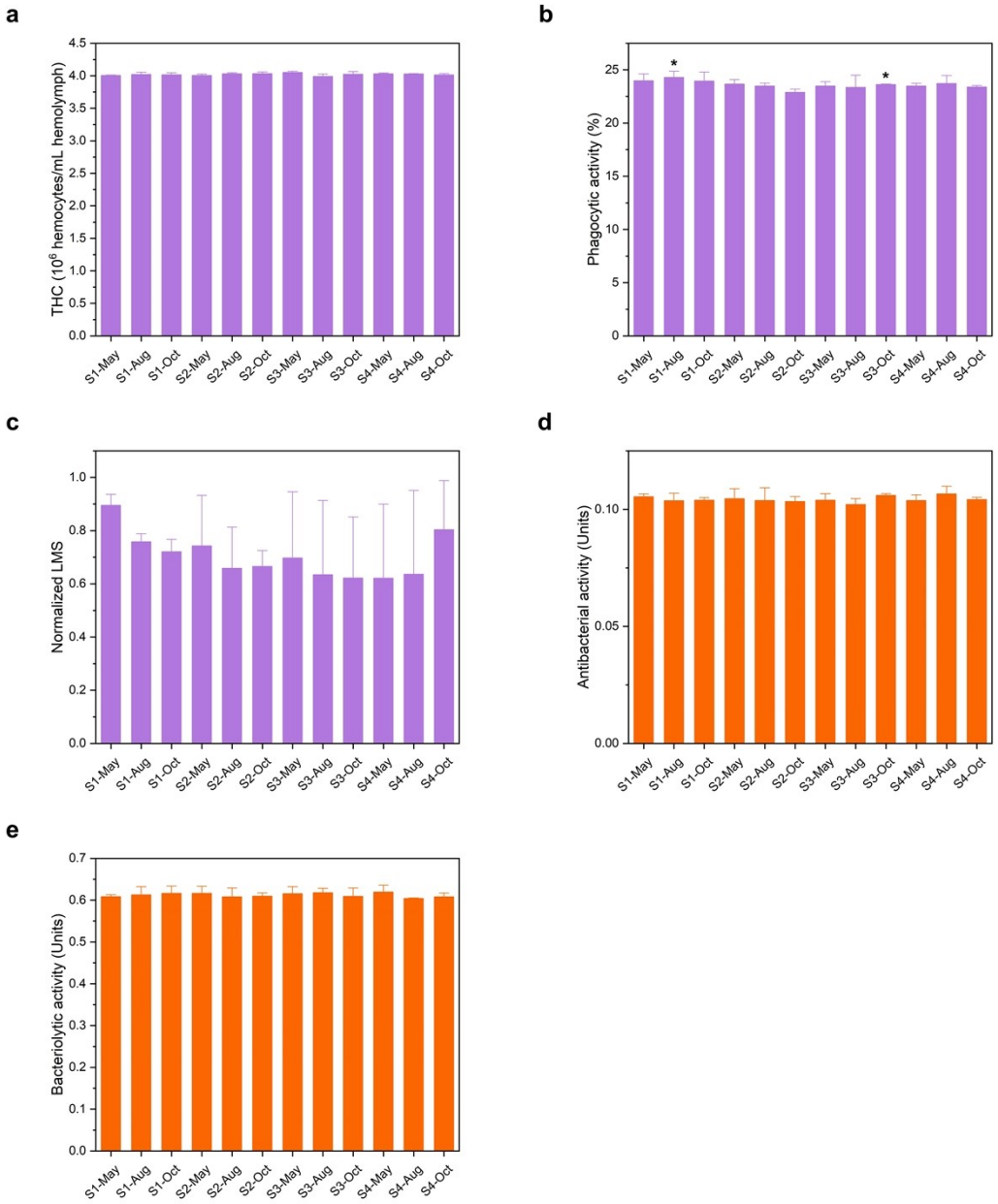

Fig. S11. The biological responses of immunotoxicity indicator: total hemocyte count (THC) (a), phagocytic activity (b), and lysosomal membrane stability (LMS) in hemocytes (purple) and antibacterial activity and bacteriolytic activity in plasma (orange) of *Ruditapes philippinarum* collected at the 4 sites in 2021. Values are presented in bar chart (n = 3). Asterisk denotes significant differences between the minimum and the other using one-way ANOVA followed by Duncan's test (*$P < 0.05$, **$P < 0.01$).

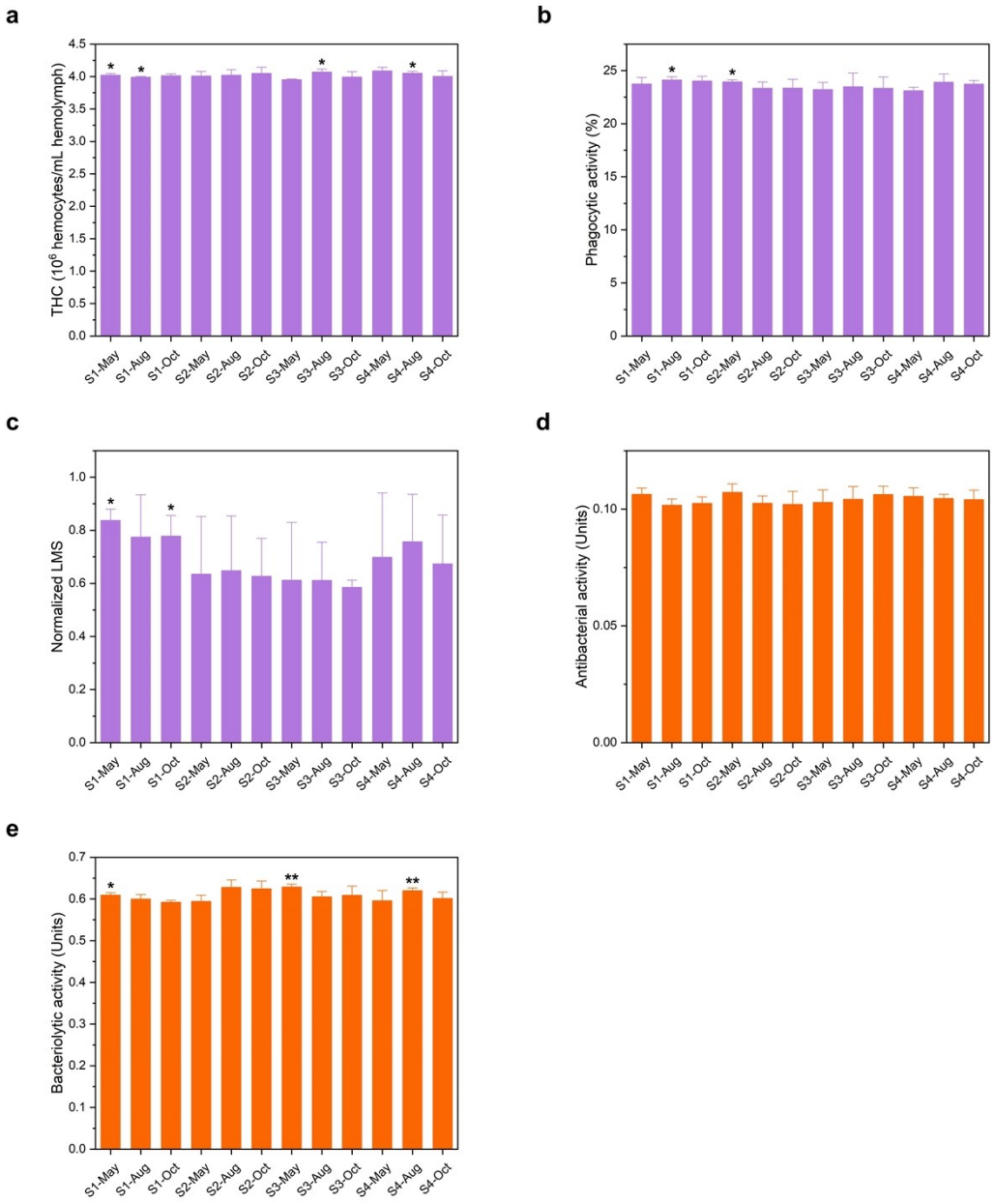

Fig. S12. The biological responses of immunotoxicity indicator: total hemocyte count (THC) (a), phagocytic activity (b), and lysosomal membrane stability (LMS) in hemocytes (purple) and antibacterial activity and bacteriolytic activity in plasma (orange) of *Mactra veneriformis* collected at the 4 sites in 2021. Values are presented in bar chart (n = 3). Asterisk denotes significant differences between the minimum and the other using one-way ANOVA followed by Duncan's test (*$P < 0.05$, **$P < 0.01$).

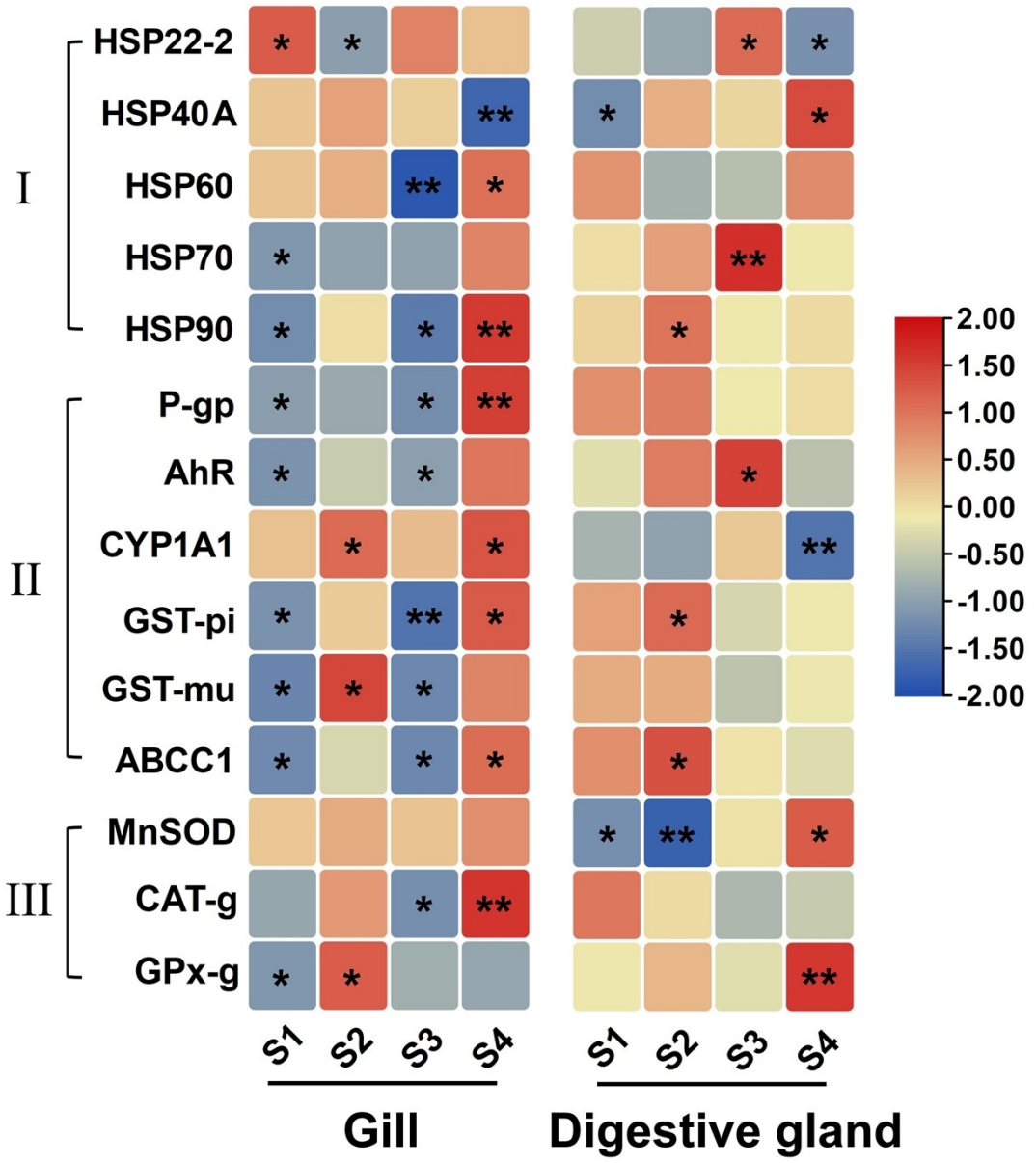

Fig. S13. The heatmap of gene expression covering stress level, detoxification and antioxidant system in the gill and digestive gland of *Ruditapes philippinarum* collected at the 4 sites in 2021, including heat shock protein (HSP22-2, 40A, 60, 70 and 90), P-glycoprotein (P-gp), aryl hydrocarbon receptor (AhR), cytochrome P450 family 1 subfamily A member 1 (CYP1A1), glutathione S-transferase (GST-pi and mu), ATP binding cassette subfamily C member 1 (ABCC1), Mn superoxide dismutase (MnSOD), catalase (CAT-g), and glutathione peroxidase (GPx-g). Values are presented in heatmap (n = 9). Asterisk denotes significant differences between the minimum and the other using one-way ANOVA followed by Duncan's test (*$P < 0.05$, **$P < 0.01$).

Supplementary References

1. The People's Republic National Standards GB/T 26411-2010. Determination of 16 polynuclear aromatic hydrocarbons in seawater by GC-MS. (2010). General Administration of Quality Supervision, Inspection and Quarantine of the People's Republic of China, Beijing, PRC.
2. The People's Republic National Standards HJ 805-2016. Soil and Sediment - Determination of polycyclic aromatic hydrocarbons by Gas chromatography-Mass Spectrometry Method. (2016). State Environmental Protection Bureau, Beijing, PRC.
3. The People's Republic National Standards GB 5009.265-2016. National Food Safety Standard - Determination of Polycyclic Aromatic Hydrocarbons in Food. (2016). China Food and Drug Administration, Beijing, PRC.
4. Otim, O. To freeze, or not to freeze: the impact of subzero temperature on quantifying organic contaminants in ocean sediments. *Environ. Sci.-Proc. Imp.*, **21**, 1580-1595 (2019).
5. Amiard, J. -C., Gefard, A. & Amiard-Triquet, C. La métallothionéine chez la moule *Mytilus edulis* comme biomarqueur de pollution métallique: variabilité entre sites, saisons et organes. *J. Rech. Oceanogr.* **23**, 25-30 (1998).
6. Bodoy, A., Prou, J. & Berthome, J. P. Etude comparative de differents indices de condition chez l'Huître Creuse (*Crassostrea Gigas*). *Haliotis* **15**, 173-182 (1986).
7. Yap, C. K., Ismail, A. & Tan, S. G. Effects of total soft tissue and shell thickness on the accumulation of heavy metals (Cd, Cu, Pb, and Zn) in the green-lipped mussel *Perna viridis*. *Russ. J. Mar Biol.* **29**, 323-327 (2003).
8. Grant, A. & Tyler, P. A. Statistical analyses in studies of invertebrate reproduction. Introduction and statistical analysis of gonad indices and maturity indices. *Int. J. Invert. Reprod*. **6**, 259-269 (1983).
9. Cartier, S. J., Pellerin, M., Fournier, É., Tami-gneaux, L. & Girault, L. Use of an index based on the blue mussel digestive gland weight in assessing environmental conditions. *Aquaculture* **241**, 633-654 (2004).
10. Pohl, R. J. & Fouts, J. R. A rapid method for assaying the metabolism of 7-ethoxyresorufin by microsomal subcellular fractions. *Anal. Biochem.* **107**, 150-155 (1980).
11. Habig, W. H., Pabst, M. J. & Jakoby, W. B. Glutathione S-transferases the first enzymatic step in mercapturic acid formation. *J. Biol. Chem.* **249**, 7130-7139 (1974).
12. Marklund, S. & Marklund, G. Involvement of the superoxide anion radical in the autoxidation of pyrogallol and a convenient assay for superoxide dismutase. *Eur. J. Biochem.* **47**, 469-474 (1974).
13. Greenwald, R. A. Handbook of Methods for Oxygen Radical Research. CRC Press, Boca Raton, FL. (1985).
14. Halliwell, B. & Gutteridge, J. M. C. Free Radicals in Biology and Medicine. Oxford Univ. Press, Oxford. (1999).
15. Wills, E. D. Evaluation of Lipid Peroxidation in Lipids and Biological Membranes. In: Snell, K., Mullock, B. (Eds.), Biochemical Toxicology. A Practical Approach. IRL Press, Oxford, pp. 127-152. (1987).
16. Lund, M. N., Lametsch, R., Hviid, M. S., Jensen, O. N. & Skibsted, L. H. High-oxygen packaging atmosphere influences protein oxidation and tenderness of porcine longissimus dorsi during chill storage. *Meat Sci.* **77**, 295-303 (2007).

17. Ellman, G. L., Courtney, K. D., Andres, V., Featherstone, R. M. A new and rapid colorimetric determination of acetylcholinesterase activity. *Biochem. Pharmacology* (Basel) **7**, 88-95 (1961).
18. Ching, E. W. K. et al. DNA adduct formation and DNA strand breaks in green-lipped mussels (*Perna viridis*) exposed to benzo a pyrene: dose- and time-dependent relationships. *Mar. Pollut. Bull.* **42**, 603-610 (2001).
19. Lin, P. F. et al. Acute and chronic toxicity effects of acrylonitrile to the juvenile marine flounder *Paralichthys olivaceus*. *Environ. Sci. Pollut. Res.* **25**, 35301-35311 (2018).
20. Bradford, M. M. A rapid and sensitive method for the quantitation of microgram quantities of protein utilizing the principle of protein-dye binding. *Anal. Biochem.* **72**, 248-254 (1976).
21. Hu, F. W., Pan, L. Q. & Jing, F. T. Effects of hypoxia on dopamine concentration and the immune response of white shrimp (*Litopenaeus vannamei*). *J. Ocean Univ. China* **8**, 77-82 (2009).
22. Yue, F., Pan, L. Q., Xie, P., Zheng, D. B, Li, J. A. Immune responses and expression of immune-related genes in swimming crab *Portunus trituberculatus* exposed to elevated ambient ammonia-N stress. *Comp. Biochem. Physiol. A* **157**, 246-251 (2010).
23. Pipe, R., Coles, J., Carissan, F. & Ramanathan, K. Copper induced immunomodulation in the marine mussel, *Mytilus edulis*. *Aquat. Toxicol.* 46, 43-54 (1999).
24. Hultmark, D., Steiner, H., Rasmuson, T., Boman, H.G. Insect immunity. Purification and properties of three inducible bactericidal proteins from hemolymph of immunized pupae of *Hyalophora cecropia*, *Eur. J. Biochem.* **106**, 7-16 (1980).
25. Schmittgen, T. D. & Livak, K. J. Analyzing real-time PCR data by the comparative CT method. *Nat. Protoc.* **3**, 1101-1108 (2008).
26. Kalf, D. F., Crommentuijn, T., & van de Plassche, E.J. Environmental quality objectives for 10 polycyclic aromatic hydrocarbons (PAHs). *Ecotoxicol. Environ. Saf.* **36**, 89-97 (1997).
27. Cao, Z. G. et al. Distribution and ecosystem risk assessment of polycyclic aromatic hydrocarbons in the Luan River, China. *Ecotoxicology* **19**, 827-837 (2010).
28. US Environmental Protection Agency (US-EPA). Guidelines for exposure assessment. EPA/600/Z-92/001. *Fed. Regist.* **57**, 22888-22938 (1992).
29. Nisbet, I.C.T. & Lagoy, P.K., 1992. Toxic equivalency factors (TEFs) for polycyclic aromatic hydrocarbons (PAHs). *Regul. Toxicol. Pharmacol.* 16, 290-300.
30. Shandong Provincial Bureau of Statistics of China. Shandong Statistics Yearbook 2022. (2022). from. http://tjj.shandong.gov.cn/tjnj/nj2022/zk/zk/indexeh.htm.
31. Wang, J., Bi, Y., Henkelmann, B., Pfister, G., Zhang, L. & Schramm, K.W. PAHs and PCBs accumulated by SPMD-based virtual organisms and feral fish in Three Gorges Reservoir, China. *Sci. Total Environ.* **542**, 899-907 (2016).
32. US Environmental Protection Agency (US-EPA). Guidance for assessing chemical contaminant data for use in fish advisories. In: Risk Assessment and Fish Consumption Limits. **2**, 1-383 (2000).
33. Beliaeff, B. & Burgeot, T. Integrated biomarker response: a useful tool for ecological risk assessment. *Environ. Toxicol. Chem.* **21**, 1316-1322 (2002).
34. Broeg, K. & Lehtonen, K. K. Indices for the assessment of environmental pollution of the Baltic Sea coasts: integrated assessment of a multi-biomarker approach. *Mar. Pollut. Bull.* **53**, 508-522 (2006).

35. Narbonne, J. F., Daubèze, M., Clérandeau, C., & Garrigues, P. Scale of classification based on biochemical markers in mussels: application to pollution monitoring in European coasts. *Biomarkers* **4**, 415-424 (1999).
36. US EPA, EPA Positive Matrix Factorization (PMF) 5.0 Fundamentals & User Guide. (2014). Online available at. https://www.epa.gov/air-research/positive-matrix-factorization-model-environmental-data-analyses.
37. Liu, Y. K. et al. Characterization and source identification of PM2.5-bound polycyclic aromatic hydrocarbons (PAHs) in different seasons from Shanghai, China. *Sci. Total Environ.* **644**, 725-735 (2018).
38. Wang, S. B., Ji, Y. Q., Zhao, J. B., Lin, Y. & Lin, Z. Source apportionment and toxicity assessment of PM2.5-bound PAHs in a typical iron-steel industry city in northeast China by PMF-ILCR. *Sci. Total Environ.* **713**, 136428 (2020).